COMPARATIVE ANALYSIS OF VARIOUS CONTINUOUS TIME DETERMINISTIC MODELS OF TUMOR-IMMUNE INTERACTIONS

by

ROBERT PAUL CHILDRESS

Presented to the Faculty of the Graduate School of
The University of Texas at Arlington in Partial Fulfillment
of the Requirements
for the Degree of

MASTER OF SCIENCE
IN MATHEMATICS

THE UNIVERSITY OF TEXAS AT ARLINGTON
December 2015

To my wife Kelsey. Thank you from now until forever

for your patience and support of my studies.

ACKNOWLEDGEMENTS

I would first like to thank Dr. Hristo Kojouharov for his profound insight, guidance, and inspiring mentorship as both a professor in the classroom and my thesis advisor. His knowledge, experience, and unwavering encouragement proved invaluable as I progressed towards the culmination of this degree.

I also wish to express my thanks to Dr. Jianzhong Su for his leadership in a superb mathematics department, Dr. Benito Chen for his inspiring teaching in multiple courses, and the remainder of the math faculty who helped shape me into the academic I am today. I am eternally grateful for the opportunities and experiences the university and department has provided me.

Though too numerous for specific mentioning, I am thankful for the many teachers, instructors, and professors at the primary, secondary, and collegiate level from whom I learned valuable wisdom and a mountain of knowledge.

Thank you to my parents for a loving home which fostered my growth to my fullest potential and for always expecting my very best. I appreciate to no end the sacrifices you made and the opportunities you afforded me to create a strong foundation upon which I have built to be where I am today.

Finally I want to give my greatest thanks to my wife. With you by my side, your unwavering support and endless encouragement fueled my motivation to persevere to the end. I cannot thank you enough. I strive to make you proud.

November 20, 2015

ABSTRACT

COMPARATIVE ANALYSIS OF VARIOUS CONTINUOUS TIME DETERMINISTIC MODELS OF TUMOR-IMMUNE INTERACTIONS

Robert Paul Childress, M.S.

The University of Texas at Arlington, 2015

Supervising Professor: Hristo Kojouharov

Cancer is historically a leading cause of death in the United States. In 2013, cancer was the second leading cause of death with 584,881 deaths [18]. Having solely been responsible for 22.5% of all deaths in 2013 alone [18], obtaining as complete an understanding as possible of cancer is obviously necessitated. This paper investigates deterministic ordinary differential equation models of increasing complexity simulating avascular tumor growth and interactions with the innate immune response. After first establishing a baseline of tumor growth resulting from the diffusion of local nutrients [5], the effects on said growth of the native immune system response, chemotherapy, immunotherapy, and various combinations of the aforementioned treatment options and responses are investigated. These efforts focus on increasing the understanding of tumor-immune interactions under various conditions and scenarios in hopes of identifying the most effective approach in combating similar cancerous tumors.

TABLE OF CONTENTS

LIST OF ILLUSTRATIONS

CHAPTER 1

INTRODUCTION

1.1 Background Information

Cancer has afflicted mankind and the animal kingdom throughout recorded history. Evidence has been discovered in fossilized bone tumors, mummified bodies, and written manuscripts of the time. Effects of the bone cancer osteosarcoma as well as cancer of the head and neck have been observed in mummified remains [37]. Though the word cancer had not been established yet, the oldest record of cancer dates back to approximately 3,000 B.C. in ancient Egypt [37]. A textbook on trauma surgery described eight cases of tumors removed from the breast. Short of brutal removal, the Egyptians remarked no available treatments for the disease [37]. Those same feelings of helplessness and frustration remain today for many modern forms of cancer. With additional research similar to that presented in this paper, perhaps all iterations of malignant cancer will one day be treatable.

Currently many treatments are available to those with cancer. Though many courses of treatment are dependent on the type and location of cancer, generally speaking, the options include surgical removal, radiation, hormone therapy, immunotherapy, chemotherapy, and targeted therapy [37]. While treatments of cancer were incredibly rudimentary and largely ineffective early in history, the treacherous stigma of cancer is pervasive even in modern society despite the innumerable advances of medicine. As such many still do not seek out treatment or consult a doctor until it is too late for successful eradication of the disease.

The key to increased survivability is accurate and, preferably, early detection. History notes, however, the unfortunate reality of cancer returning upon cessation of treatment. With early detection being so important, it begs the question of what options are available if detection methods and tests determine the prescence of cancer, either initially or even after a full course of treatment for existing cancer, but the exact location of the burgeoning tumor is not known. For example, a test might return conclusive results regarding the existence of cancer cells in the body, but perhaps the tumor is too infantile to be seen on image screens or the like. In such a situation, the use of many location-specific treatment options are obviously limited.

Such situations are indicative of avascular tumors, i.e. those which are small enough to be without a native vascular system within the cancerous growth itself through which to transport important nutrients but large enough to be problematic and require treatment. Instead such tumors resude adjacent to a viable nutrient source, i.e. local blood vessel, from which to diffuse nutrients required for growth [17], [5]. The aforementioned inherent differences from more mature cancerous growths demand specific research and methods into the respective treatment of these type tumors.

1.2 Structure of Paper

Motivated by the differences in treatment methods necessitated by the distinct attributes and behavior of an avascular tumor, this paper investigates varying treatment models and their respective levels of success. In Chapters 2 through 5, models are discussed from the simplest, growth-only model to the most complex model analyzed with multiple models of intermediate complexity along the way.

Each model is introduced and described with its motivating reasoning, interaction diagrams, a brief description of the mechanics at work, respective equation(s),

stability analysis of equilibrium points where possible, and graphs of varying numerical simulations. Chapter 5 establishes the most efficient model discussed and investigates slight variations of that model in hopes of increasing its effectiveness even more. Discussion is had regarding further and future extensions of this study and questions to be answered.

1.3 Implementation of Models

Depending on the inherent complexity of each model, some are implemented in a scaffolded fashion when appropriate. First the foundational model of tumor-immune interactions is presented, then a drug therapy term is introduced, followed by an immunotherapy term, and then finally both external treatments are combined to investigate the overall effects of the respective treatments in that particular model. Each respective model and submodel is additionally analyzed for stationary points and corresponding stability. All efforts are conducted with the goal of identifying either a specific model or class of models which most effectively combats the cancer tumor.

CHAPTER 2

TUMOR GROWTH ONLY

2.1 Motivating the Model

The first model presented is a logistical growth model representative of an avascular tumor unaffected by any immune response, native or external of the body. This growth model was first presented in 1838 by Pierre François Verhulst [21] as he was researching population growths and studying the works of Thomas R. Malthus [29] and his compatriot Adolphe Quetelet [35]. It still remains a popular and accurate model representing population dynamics. The interaction diagram below provides a visual representation of the actions portrayed by this respective model.

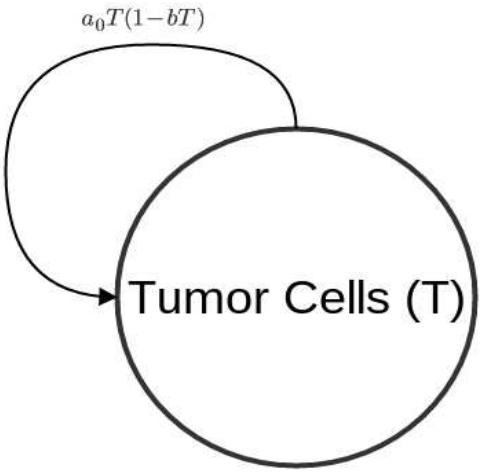

Figure 2.1: Growth Only Interaction Diagram

Increasing by the growth rate a_0, this model of tumor growth serves as a baseline of nutrient diffusion-restrained amassment until the tumor reaches its limiting population of $\frac{1}{b}$, where b represents the inverse maximum population value. One can easily see as T nears the value of $\frac{1}{b}$, the latter half of the growth term, i.e. $(1 - bT)$, will tend towards 0 thus ensuring the entire growth expression tends towards 0 and stops the tumor growth entirely. Putting it all together yields the following single equation, logistical growth model:

$$\frac{dT}{dt} = a_0 T(1 - bT) \tag{2.1}$$

2.2 Analysis of the Model

Finding equilibrium points of the model, Equation (2.1) is first set equal to zero and solved for the variable T.

$$a_0 T(1 - bT) = 0 \tag{2.2}$$

$$a_0 T = 0 \qquad\qquad 1 - bT = 0 \tag{2.3}$$

$$T_0^* = 0 \qquad\qquad T_1^* = \frac{1}{b} \tag{2.4}$$

With the two equilibrium points having been found, the stability of each respective point needs establishing. Because the current model is comprised of a single equation, the stability is found by taking the first derivative of $\frac{dT}{dt}$ with respect to the

variable T and then evaluating that derivative equation at each equilibrium point, T_0^* and T_1^*. Let $T' = \frac{dT}{dt}$.

$$\frac{dT'}{dT} = a_0 T(-b) + a_0(1 - bT) \tag{2.5}$$

$$= -a_0 bT + a_0 - a_0 bT \tag{2.6}$$

$$= -2a_0 bT + a_0 \tag{2.7}$$

$$= -a_0(2bT - 1) \tag{2.8}$$

Evaluating Equation (2.8) at T_0^* yields $\frac{dT'}{dT} = a_0$. Because a_0 represents the tumor growth rate and $a_0 > 0$, $\frac{dT'}{dT}(T_0^*) > 0$, thus indicating T_0^* as unstable. The tumor cell population is growing away from $T_0^* = 0$.

Evaluating Equation (2.8) at T_1^* yields $\frac{dT'}{dT} = -a_0$. Because a_0 represents the tumor growth rate and $a_0 > 0$, $\frac{dT'}{dT}(T_1^*) < 0$, thus indicating T_0^* as stable. The tumor cell population is trending towards $T_1^* = \frac{1}{b}$.

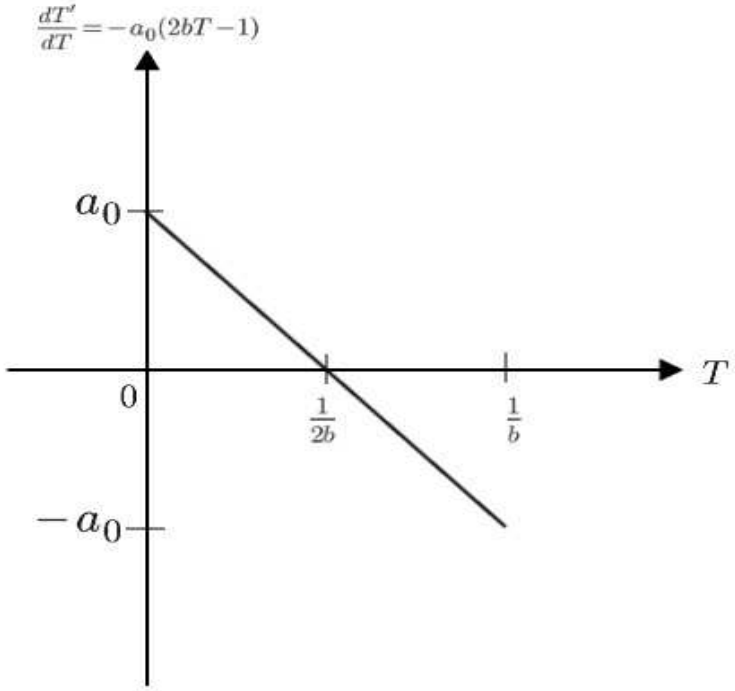

Figure 2.2: Graph of $\frac{dT'}{dT}$

Figure (2.4) demonstrates the linear function of the rate of change of the tumor cell population over time versus the tumor cell population itself, i.e. $\frac{dT'}{dT}$. At $T = 0$ Equation (2.8) has a value of a_0. At $T = \frac{1}{2b}$ the same equation has a value of 0. Then at $T = \frac{1}{b}$ the equation has a value of $-a_0$.

2.3 Numerical Simulation

Solving the above model in MATLAB using ode45 with initial values of $T_0 = 3 \times 10^7$ for tumor cell population [24], $a_0 = 0.13$ for tumor cell growth [24], and $b = 2.3 \times 10^{-10}$ for inverse tumor cell limiting population [24] we see the numerical

simulation as follows. See Table A.1 for additional information regarding the model's initial values and parameter values.

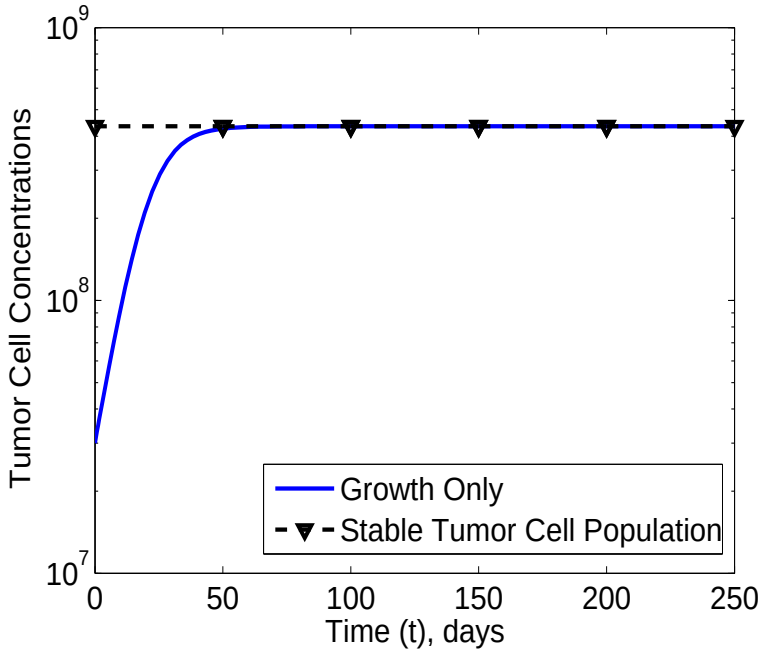

Figure 2.3: Growth Only

The results of the numerical simulation match those as expected from the stability analysis previously performed with the appropriately defined initial conditions. The simulation grows away from $T = 0$ and tends towards the maximum tumor cell population value represented by $\frac{1}{b}$ where $T = 4.35 \times 10^8$. The next logical step in increasing the complexity of the model is to introduce native immune cells via a competition term with the tumor cells and then observe the effects on the model.

CHAPTER 3

TUMOR-IMMUNE I

3.1 Base Model

3.1.1 Motivating the Model

This model represent the first interactions between the growing tumor and the innate immune system of the host organism. The tumor grows according to the previously established growth term but is also lessened by the activity of the immune response, specifically cytotoxic T cells.

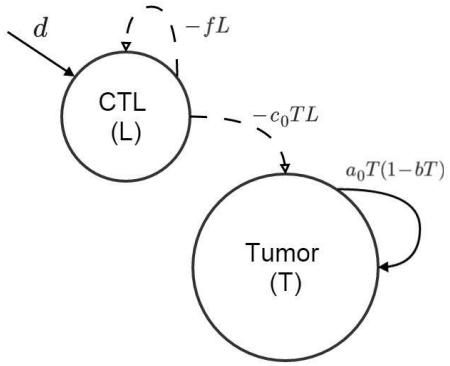

Figure 3.1: Tumor-Immune I - Base Model Interaction Diagram

The immune response, represented by L and modeling CTL (cytotoxic T) cells, is increased at a steady influx rate represented by the variable d but also decreased as a result of natural decay as represented by the variable f. The tumor cells are modeled by the same growth term as before but are also decreased by the interactions

with the immune system cells as represented by the term $-c_0TL$ where c_0 is the tumor cell kill rate [24]. These interactions involve the immune system CTL cells finding and attacking the tumor cells. This basic tumor-immune system forms the following two-equation model:

$$\frac{dT}{dt} = a_0T(1 - bT) - c_0TL \tag{3.1}$$

$$\frac{dL}{dt} = d - fL \tag{3.2}$$

3.1.2 Analysis of the Model

Finding equilibrium points of this two-equation model, the simultaneous Equations (3.1) and (3.2) are first set equal to zero and solved for the respective variables T and L.

$$\frac{dT}{dt} = a_0T(1 - bT) - c_0TL = 0 \qquad \frac{dL}{dt} = d - fL = 0 \tag{3.3}$$

$$T[a_0(1 - bT) - c_0L] = 0 \qquad fL = d \tag{3.4}$$

$$T = 0 \qquad a_0(1 - bT) - c_0L = 0 \qquad L = \frac{d}{f} \tag{3.5}$$

$$1 - bT = \frac{c_0L}{a_0} \tag{3.6}$$

$$bT = 1 - \frac{c_0L}{a_0} \tag{3.7}$$

$$bT = \frac{a_0 - c_0L}{a_0} \tag{3.8}$$

$$T = \frac{a_0 - c_0L}{a_0b} \tag{3.9}$$

Substituting $\frac{d}{f}$ for L in Equation (3.9) produces the following two equilibrium points:

$$T_0^* = 0 \qquad L_0^* = \frac{d}{f} \tag{3.10}$$

and

$$T_1^* = \frac{a_0 f - c_0 d}{a_0 b f} \qquad L_1^* = \frac{d}{f} \tag{3.11}$$

Let E_0^* be the first equilibrium point containing L_0^* and T_0^*, and let E_1^* be the second equilibrium point containing L_1^* and T_1^*. Having found the two equilibrium points of the model, the respective stability of E_0^* and E_1^* requires establishing. As such, partial derivatives of each model equation, i.e. Equations (3.1) and (3.2), are found with respect to each variable T and L. With these partial derivative expressions, the Jacobian of the system is created. Evaluating the Jacobian matrix at each equilibrium point, respective eigenvalues are then computed. The stability of each equilibrium point is described by the signs of each pair of resulting eigenvalues. Let $T' = \frac{dT}{dt}$, and let $L' = \frac{dL}{dt}$.

$$\frac{\partial T'}{\partial T} = a_0 T(-b) + a_0(1 - bT) - c)L \tag{3.12}$$

$$= -a_0(2bT - 1) - c_0 L \tag{3.13}$$

$$\frac{\partial T'}{\partial L} = -c_0 T \tag{3.14}$$

$$\frac{\partial L'}{\partial T} = 0 \tag{3.15}$$

$$\frac{\partial L'}{\partial L} = -f \tag{3.16}$$

Let J be the Jacobian of the system. J_0 represents the Jacobian matrix evaluated at the first equilibrium point, E_0^*.

$$J = \begin{bmatrix} \frac{\partial T'}{\partial T} & \frac{\partial T'}{\partial L} \\ \frac{\partial L'}{\partial T} & \frac{\partial L'}{\partial L} \end{bmatrix} = \begin{bmatrix} -a_0(2bT-1) - c_0 L & -c_0 T \\ 0 & -f \end{bmatrix} \tag{3.17}$$

$$J_0 = \begin{bmatrix} a_0 - \frac{c_0 d}{f} & 0 \\ 0 & -f \end{bmatrix} \tag{3.18}$$

The next step in solving for the eigenvalues of J_0 is finding the determinant of the matrix created by the difference $J_0 - \lambda I$, where I is the appropriately sized identity matrix. The determinant then creates the characteristic equation from which the eigenvalues can be solved.

$$J_0 - \lambda I = \begin{bmatrix} a_0 - \frac{c_0 d}{f} - \lambda & 0 \\ 0 & -f - \lambda \end{bmatrix} \tag{3.19}$$

$$det(J_0 - \lambda I) = 0 \tag{3.20}$$

$$(a_0 - \frac{c_0 d}{f} - \lambda)(-f - \lambda) = 0 \tag{3.21}$$

$$\lambda_1 = -f \tag{3.22}$$

$$\lambda_2 = a_0 - \frac{c_0 d}{f} \tag{3.23}$$

The equilibrium point E_0^* is stable when both λ_1 and λ_2 have negative real parts, i.e. when $f > 0$ and $a_0 < \frac{c_0 d}{f}$. The equilibrium point E_0^* is unstable when either λ_1 or λ_2 has positive real parts, i.e. $f < 0$ or $a_0 > \frac{c_0 d}{f}$. In a biological context, f is a decay rate and will always be positive in the scope of this model. Therefore the stability of E_0^* depends upon the sign of λ_2 and how it may change relative to the parameter values used in the model.

With $\lambda_2 = a_0 - \frac{c_0 d}{f}$, the equilibrium point E_0^* will be stable when the tumor growth rate, a_0, is less than the product of the constant influx of immune cells, d, and the tumor-immune competition coefficient, c_0, divided by the immune cell decay rate, f. Alternatively, E_0^* will be unstable when the tumor growth rate is greater than the product of the constant influx of immune cells and the tumor-immune competition term divided by the immune cell decay rate.

Having found the respective eigenvalues for E_0^*, the process is repeated for the second equilibrium point, E_1^*. Using the same Jacobian matrix, J, from above, J_1 represents the Jacobian matrix evaluated at E_1^*.

$$J = \begin{bmatrix} -a_0(2bT-1) - c_0L & -c_0T \\ 0 & -f \end{bmatrix} \tag{3.24}$$

$$J_1 = \begin{bmatrix} -a_0[2b(\frac{a_0f-c_0d}{a_0bf}) - s] - \frac{c_0d}{f} & -c_0(\frac{a_0f-c_0d}{a_0bf}) \\ 0 & -f \end{bmatrix} \tag{3.25}$$

$$= \begin{bmatrix} \frac{-2a_0f+c_0d+a_0f}{f} & \frac{-c_0a_0f+{c_0}^2d}{a_0bf} \\ 0 & -f \end{bmatrix} \tag{3.26}$$

$$= \begin{bmatrix} \frac{-2a_0f+c_0d+a_0f}{f} & \frac{-c_0a_0f+{c_0}^2d}{a_0bf} \\ 0 & -f \end{bmatrix} \tag{3.27}$$

As before, the next step in solving for the eigenvalues of J_1 is finding its respective determinant. This process then gives rise to the characteristic equation from which the eigenvalues can be calculated.

$$J_1 - \lambda I = \begin{bmatrix} \frac{-2a_0f+c_0d+a_0f}{f} - \lambda & \frac{-c_0a_0f+{c_0}^2d}{a_0bf} \\ 0 & -f-\lambda \end{bmatrix} \tag{3.28}$$

$$det(J_1 - \lambda I) = 0 \tag{3.29}$$

$$(\frac{-2a_0f + c_0d + a_0f}{f} - \lambda)(-f-\lambda) = 0 \tag{3.30}$$

$$\lambda_1 = \frac{c_0d}{f} - a_0 \tag{3.31}$$

$$\lambda_2 = -f \tag{3.32}$$

The equilibrium point E_1^* is stable when both λ_1 and λ_2 have negative real parts, i.e. when $f > 0$ and $a_0 > \frac{c_0 d}{f}$. The equilibrium point E_1^* is unstable when either λ_1 or λ_2 has positive real parts, i.e. $f < 0$ or $a_0 < \frac{c_0 d}{f}$. As previously mentioned, f is a decay rate and will always be positive in the scope of this model. Therefore the sign of λ_2 and how it changes relative to the parameter values used in the model determines the stability of E_1^*.

The equilibrium point E_1^* essentially has the opposite behavior as the previous equilibrium point, E_0^*: it is stable when the tumor growth rate, a_0, is greater than the product of the constant influx of immune cells, d, and the tumor-immune competition coefficient, c_0, divided by the immune cell decay rate, f. E_1^* is then unstable when the tumor growth rate is less than the product of the constant influx of immune cells and the tumor-immune competition term divided by the immune cell decay rate.

3.1.3 Numerical Simulation

Solving the above model in MATLAB using ode45 with initial values of $T_0 = 3 \times 10^7$ for tumor cell population [24], $a_0 = 0.13$ for tumor cell growth [24], $b = 2.3 \times 10^{-10}$ for inverse tumor cell limiting population [24], $c_0 = 4.4 \times 10^{-9}$ as the competition coefficient between tumor cells and immune system cells [24], $d = 7.3 \times 10^6$ for the constant influx rate of immune system cells [24], and $f = 0.33$ for the decay rate of immune cells [24], the numerical simulation is as follows. See Table A.1 for additional information regarding the model's initial values and parameter values.

The results of the numerical simulation match those as expected from the stability analysis previously performed in the chapter with the appropriately defined initial conditions. The parameter values used ($a_0 = 0.13$, $c_0 = 4.4 \times 10^{-9}$, $d = 7.3 \times 10^6$, and $f = 0.33$) correspond to E_0^* being unstable with eigenvalues $\lambda_1 = -f = -0.33$

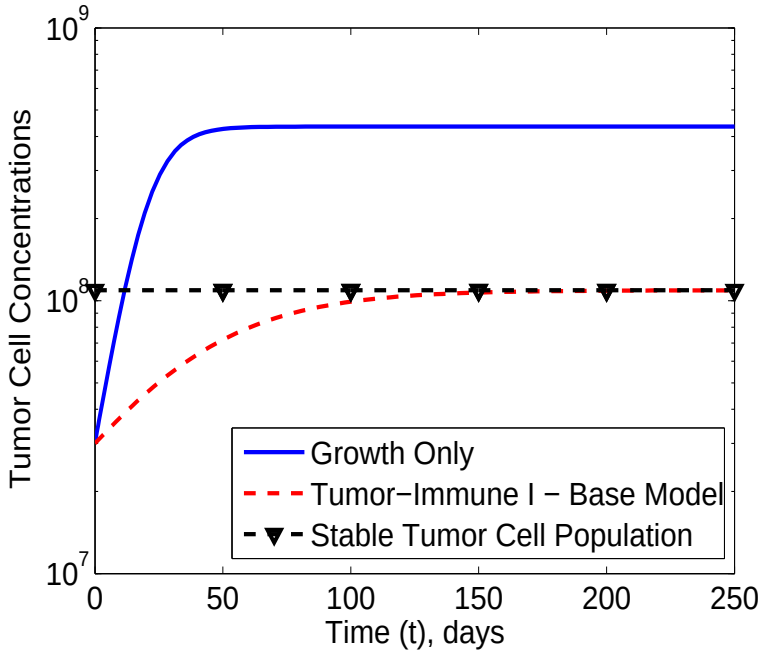

Figure 3.2: Tumor-Immune I - Base Model

and $\lambda_2 = a_0 - \frac{c_0 d}{f} = 0.33$ thus causing the tumor cell population to increase away from $T = 0$. Conversely the parameter values correspond to E_1^* being stable with eigenvalues $\lambda_1 = -f = -0.33$ and $\lambda_2 = \frac{c_0 d}{f} - a_0 = -0.0327$ thus causing the tumor cell population to trend towards $T_1^* = \frac{a_0 f - c_0 d}{a_0 b f} = 1.0925 \times 10^8$.

Investigating the alternative scenario, however, the parameter values are adjusted in a way remaining logical to the biological mechanics at hand such that the stability of the equilibrium points should reverse. The numerical simulation below reflects this change as the immune cell induction rate increases to $d = 7.3 \times 10^7$.

As evidenced by the graph in Figure (3.3), the stability of the two equilibrium points reverses. The immune cell induction rate is the only parameter changed, and it realized an increase to $d = 7.3 \times 10^7$ from its original value of $d = 7.3 \times 10^6$. All of the remaining parameters remain constant to their original values ($a_0 = 0.13$, $c_0 = 4.4 \times 10^{-9}$, and $f = 0.33$). E_0^* is now stable with its corresponding eigenvalues

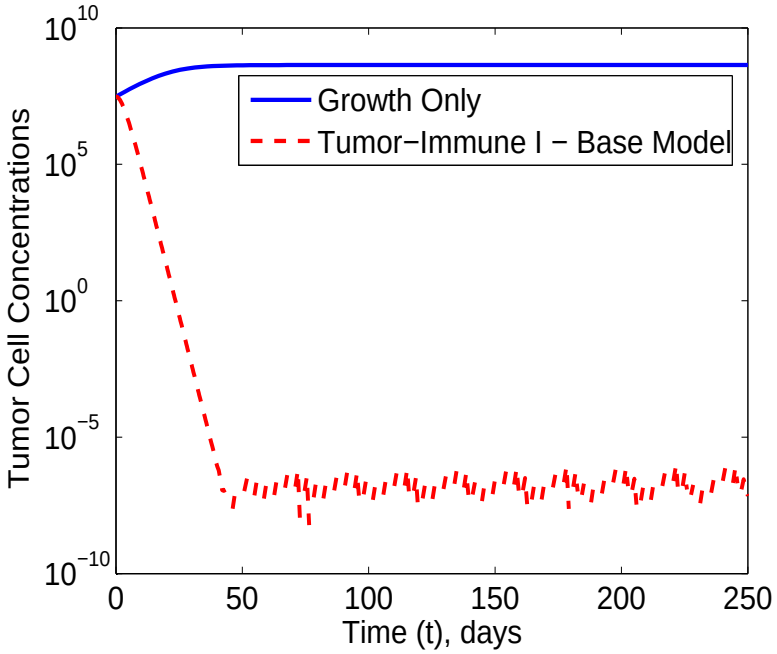

Figure 3.3: Tumor-Immune I - Base Model

of $\lambda_1 = -f = -0.33$ and $\lambda_2 = a_0 - \frac{c_0 d}{f} = -0.8433$ causing the tumor cell population to decrease towards $T_0^* = 0$. E_1^* is now unstable with its respective eigenvalues of $\lambda_1 = -f = -0.33$ and $\lambda_2 = \frac{c_0 d}{f} - a_0 = 0.8433$ causing the tumor cell population to decrease away from $T_1^* = \frac{a_0 f - c_0 d}{a_0 b f} = 1.0925 \times 10^8$.

The next step in the progression of this model is to introduce a chemotherapy term and investigate its effects on both the tumor cell and immune cell populations.

3.2 Drug Therapy

3.2.1 Motivating the Model

This next model is a variation of the preceeding one in that all the cell interactions remain constant but differs in results as external drugs in the form of chemotherapy are introduced into the model dynamics. The chemotherapy affects both the tumor cells and native immune cells albeit at differing rates. That is, the

chemotherapy has a higher kill rate of tumor cells than immune cells as one would hope and expect for successful treatment. The chemotherapy is time-dependent, meaning it is introduced at a constant rate for only so many days before the intake supply is turned off for protection of the patient. This is a reasonable expectation since the chemotherapy drugs affect not only the tumor cells but also the immune cells as previously discussed. The chemotherapy also has a decay rate of its own, so after a sufficient amount of time post cessation of drug intake, the model returns to the steady state behavior of the preceeding model involving only basic interactions between the tumor and native immune system. Despite being time-dependent and alternating between being active and inactive for a period of time as the model is implemented, for the purposes of model analysis the drug therapy induction rate is considered a constant value.

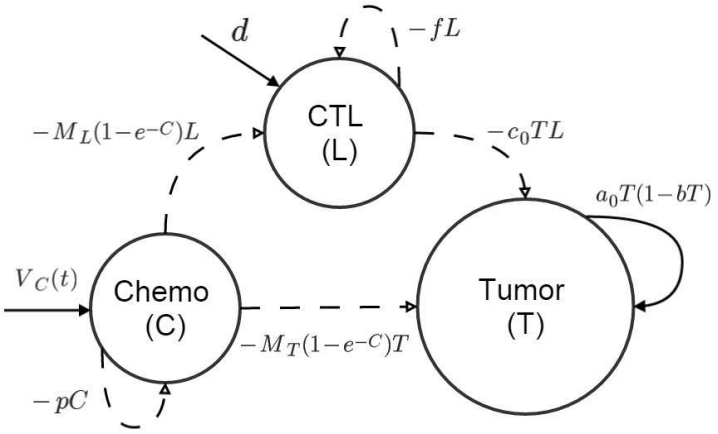

Figure 3.4: Tumor-Immune I - Drug Therapy Interaction Diagram

As seen in the interaction diagram, this model varies only slightly from the previous one in that chemotherapy terms are now added. All other terms of the established tumor and immune cell equations remain. The chemotherapy concentration

is represented by the variable C. The drug is introduced via time-dependent function $V_C(t)$. When active, the rate of introduction is a positive constant, and when inactive the rate is zero. The drug decays by a rate represented by the variable p. The chemotherapy affects both the tumor cells and immune cells at respective kill rates of M_T and M_L. These rates, however, decrease in effectiveness as the concentration of chemotherapy drugs lessens as represented by the $1 - e^{-C}$ term in both tumor and immune cell equations.

$$\frac{dT}{dt} = a_0T(1 - bT) - c_0TL - M_T(1 - e^{-C})T \tag{3.33}$$
$$\frac{dL}{dt} = d - fL - M_L(1 - e^{-C})L \tag{3.34}$$
$$\frac{dC}{dt} = V_C(t) - pC \tag{3.35}$$

3.2.2 Analysis of the Model

Following the established pattern, the first step in analyzing the model is finding the equilibrium points. This is accomplished by solving the three-equation system for each variable representing the tumor cells, immune cells, and chemotherapy concentration. For purposes of solving the system, the intake function for chemotherapy is treated as a constant.

$$\frac{dT}{dt} = a_0T(1 - bT) - c_0TL - M_T(1 - e^{-C})T = 0 \tag{3.36}$$
$$\frac{dL}{dt} = d - fL - M_L(1 - e^{-C})L = 0 \tag{3.37}$$
$$\frac{dC}{dt} = V_C - pC = 0 \tag{3.38}$$

To simplify the analysis of the system, the equations are coded into a MATLAB script. The time-dependency notation of the drug induction rate, V_C, is dropped, and it is treated as a constant in the calculations. The resulting equilibrium points are as follows:

$$T_0^* = \frac{-\left(M_T - a_0 - M_T e^{\frac{-V_C}{p}} + \frac{c_0 * d}{f - M_L(e^{\frac{-V_C}{p}} - 1)}\right)}{a_0 b} \tag{3.39}$$

$$L_0^* = \frac{d}{f - M_L(e^{\frac{-V_C}{p}} - 1)} \tag{3.40}$$

$$C_0^* = \frac{V_C}{p} \tag{3.41}$$

and

$$T_1^* = 0 \tag{3.42}$$

$$L_1^* = \frac{d}{f - M_L(e^{\frac{-V_C}{p}} - 1)} \tag{3.43}$$

$$C_1^* = \frac{V_C}{p} \tag{3.44}$$

Let E_0^* be the first equilibrium point containing T_0^*, L_0^*, and C_0^*, and let E_1^* be the second equilibrium point containing T_1^*, L_1^*, and C_1^*. Investigating the stability of each equilibrium point again requires a partial derivative to be taken of each model equation with respect to each of the three main component variables: T, L, and C. With these partial derivative expressions, the Jacobian of the system is created. Evaluating the Jacobian matrix at each equilibrium point E_0^* and E_1^*, respective eigenvalues are then computed. The stability of each equilibrium point is described by the signs of each group of resulting eigenvalues.

Let $T' = \frac{dT}{dt}$.

$$\frac{\partial T'}{\partial T} = -a_0(2bT - 1) - c_0 L - M_T(1 - e^{-C}) \tag{3.45}$$
$$\frac{\partial T'}{\partial L} = -c_0 T \tag{3.46}$$
$$\frac{\partial T'}{\partial C} = -M_T T e^{-C} \tag{3.47}$$

Let $L' = \frac{dL}{dt}$.

$$\frac{\partial L'}{\partial T} = 0 \tag{3.48}$$
$$\frac{\partial L'}{\partial L} = -f - M_L(1 - e^{-C}) \tag{3.49}$$
$$\frac{\partial L'}{\partial C} = -M_L L e^{-C} \tag{3.50}$$

Let $C' = \frac{dC}{dt}$.

$$\frac{\partial C'}{\partial T} = 0 \tag{3.51}$$
$$\frac{\partial C'}{\partial L} = 0 \tag{3.52}$$
$$\frac{\partial C'}{\partial C} = -p \tag{3.53}$$

Let J be the Jacobian of the system. J_0 represents the Jacobian matrix evaluated at the first equilibrium point, E_0^*.

$$J = \begin{bmatrix} \frac{\partial T'}{\partial T} & \frac{\partial T'}{\partial L} & \frac{\partial T'}{\partial C} \\ \frac{\partial L'}{\partial T} & \frac{\partial L'}{\partial L} & \frac{\partial L'}{\partial C} \\ \frac{\partial C'}{\partial T} & \frac{\partial C'}{\partial L} & \frac{\partial C'}{\partial C} \end{bmatrix} \tag{3.54}$$

$$J = \begin{bmatrix} -a_0(2bT-1) - c_0 L - M_T(1-e^{-C}) & -c_0 T & -M_T T e^{-C} \\ 0 & -f - M_L(1-e^{-C}) & -M_L L e^{-C} \\ 0 & 0 & -p \end{bmatrix} \tag{3.55}$$

Wanting again to simplify the evaluation of the Jacobian matrix J at the first equilibrium point E_0^*, the calculations and substitutions are performed in MATLAB to not only find J_0 but also the subsequent eigenvalues. As such, the eigenvalues of J_0 are as follows:

$$\lambda_1 = -p \tag{3.56}$$

$$\lambda_2 = M_L(\mathrm{e}^{-\frac{V_C}{p}} - 1) - f \tag{3.57}$$

$$\lambda_3 = \{\text{symbolic expression is of excessive length}\} \tag{3.58}$$

While the first two eigenvalues are expressed in a simple symbolic form, the third eigenvalue is a complex expression involving many terms. For succinctness the entire third eigenvalue expression is omitted.

Presented above is an interesting situation. The model is no longer autonomous as the variable V_C representing the drug therapy induction rate is time dependent.

This particular facet of the model creates two different situations on which to perform analysis: one when the drug therapy is active with V_C having a positive, non-zero constant value and another when the drug therapy is inactive and V_C is zero.

Analyzing first the stability of the situation where the drug therapy is active, it is plainly seen that λ_1 will always be negative because p is the chemotherapy decay rate, and $p > 0$ in this model. The sign of λ_2 will always be negative due to the $e^{-\frac{V_C}{p}} - 1$ expression in the first term. Because V_C and p have already been established as being both positive, $e^{-\frac{V_C}{p}} < 1$ thus forcing $e^{-\frac{V_C}{p}} - 1 < 0$. The resulting negative value multiplied onto M_L, where $M_L > 0$ always in this model, subtracted by the parameter f, the immune cell death rate where $f > 0$ for the entire model, will always result in a negative overll evaluation for the second eigenvalue. Because the first two eigenvalues proved negative, the stability of E_0^* when the drug therapy is active is decided by the third eigenvalue. Unfortunately λ_3 contains an expression proving difficult to analyze symbolically, and very likely the parameter values are necessary to make the expression more useful.

Since no absolute conclusion is reached after analyzing the symbolic expressions, the parameter values are substituted to calculate numerical expressions of the eigenvalues. Utilizing MATLAB to aid in the calculations, the following values are used: $a_0 = 0.13$ [24], $b = 2.3 \times 10^{-9}$ [24], $c_0 = 4.4 \times 10^{-9}$ [24], $d = 7.3 \times 10^6$ [24], $f = 0.33$ [24], $M_L = 0.6$ [24], $M_T = 0.9$ [24], $p = 6.4$ [24], and $V_C = 1$ [24]. These model parameters for when the chemotherapy is active yield the following eigenvalues:

$$\lambda_1 = -6.4000 \tag{3.59}$$

$$\lambda_2 = -0.3300 \tag{3.60}$$

$$\lambda_3 = 1.1262 \tag{3.61}$$

As expected, the first and second eigenvalues are negative, but the third eigenvalue is positive. This is a logical result, however, since the two equilibrium points, E_0^* and E_1^*, differ only in values for T, and this first equilibrium point, E_0^*, contains the non-zero expression for T, the tumor cell population. The expectation is that an effective drug therapy would cause the tumor population to decrease towards zero as opposed to being ineffective and seeing the tumor cell population continue towards a non-zero stable population. As such, E_0^* is an unstable equilibrium point when the chemotherapy is active ($V_C = 1$).

Analyzing the stability of the second situation where the drug therapy is inactive ($V_C = 0$), the updated value of the drug therapy induction rate significantly simplifies the eigenvalue expressions to the following:

$$\lambda_1 = -p \tag{3.62}$$

$$\lambda_2 = -f \tag{3.63}$$

$$\lambda_3 = \frac{-2da_0^2b^2 + fa_0^2b - fa_0c_0 + dc_0^2}{a_0bf} \tag{3.64}$$

It is still easily seen that the first eigenvalue will remain negative since $p > 0$ for the entire model. The second eigenvalue, however, is now significantly easier to analyze in its current symbolic state due to $V_C = 0$. The new value of V_C causes the entire first term of the expression to go to 0, leaving only the $-f$ in the entire expression. The second eigenvalue again follows in the footsteps of the first and is easily seen to always be negative since f represents the immune cell death rate and

$f > 0$ for the entire model. With both of the first two eigenvalues being negative, the stability of E_0^* when $V_C = 0$ is determined again by the sign of the third eigenvalue. Despite having been simplified greatly, the resulting symbolic expression is still inconclusive with regard to its eventual sign and effect on the overall stability of E_0^*.

Returing to numerical results of the eigenvalues to indicate the stability, the same model parameters as before are substituted save for $V_C = 0$ to indicate the drug therapy is inactive. MATLAB yields the following eigenvalues:

$$\lambda_1 = -6.4000 \tag{3.65}$$

$$\lambda_2 = -0.3300 \tag{3.66}$$

$$\lambda_3 = -0.3639 \tag{3.67}$$

The first and second eigenvalues are again negative just as projected in the preceeding analysis. This time, however, the third eigenvalue is also negative indicating E_0^* to be stable when the chemotherapy is inactive ($V_C = 0$). This is once again a logical result since without the drug therapy the tumor cells will continue to proliferate up to the non-zero stable population level of the respective equilibrium point.

Having established the stability of the first equilibrium point, E_0^*, for both cases of drug therapy, the focus now shifts to investigating the same situations for the second equilibrium point, E_1^*. Starting with the original Jacobian matrix J, evaluating J at E_1^* yields the matrix J_1. MATLAB is used again to simplify the evaluations and substitutions in finding J_1 and its related eigenvalues. As such, the eigenvalues corresponding to E_1^* are as follows:

$$\lambda_1 = -p \tag{3.68}$$

$$\lambda_2 = M_L(\mathrm{e}^{-}\frac{V_C}{p} - 1) - f \tag{3.69}$$

$$\lambda_3 = \{\text{symbolic expression is of excessive length}\} \tag{3.70}$$

Just as with the symbolic eigenvalues for E_0^*, while the first two eigenvalues are expresed in a simple symbolic form, the third eigenvalue is a complex expression involving many more terms. With brevity in mind, the entire third eigenvalue expression is again omitted.

With the time-dependent variable V_C still present in the expressions, the model remains non-autonomous. This again creates two different situations on which to perform analysis: one when the drug therapy is active with V_C having a positive, non-zero constant value and another when the drug therapy is inactive and V_C is zero.

Analyzing first the situation when the drug therapy is active, the first two eigenvalue expressions are identical to those previously seen with regards to E_0^* with the drug therapy active. The symbolic analysis thus remains the same, and the first two eigenvalues are expected to return negative values once the parameter values are substituted. With the third eigenvalue's symbolic expression being overly large, any symbolic analysis is difficult and encourages the use of MATLAB to arrive at a numerical result. Therefore, the same parameter values used before (including $V_C = 1$ to indicate the active chemotherapy) are substituted into the three eigenvalue expressions for the E_1^* equilibrium point.

$$\lambda_1 = -6.4000 \tag{3.71}$$

$$\lambda_2 = -0.4168 \tag{3.72}$$

$$\lambda_3 = -0.0107 \tag{3.73}$$

All eigenvalues corresponding to E_1^* with the drug therapy active returned a negative result, indicating E_1^* is a stable equilibrium point. This follows logical reasoning since the E_1^* equilibrium point contains $T_1^* = 0$. An effective drug therapy should force the tumor cell population to decrease towards 0, and this treatment accomplishes that goal.

Looking back at the E_1^* eigenvalue symbolic expressions for the second situation where the drug therapy is inactive and $V_C = 0$, the symbolic expressions do simplify in nature similar to that which occured for the E_0^* eigenvalue expressions.

$$\lambda_1 = -p \tag{3.74}$$

$$\lambda_2 = -f \tag{3.75}$$

$$\lambda_3 = \frac{a_0 f - 2a_0 bd}{f} \tag{3.76}$$

$$= a_0 - \frac{2a_0 bd}{f} \tag{3.77}$$

The first two eigenvalue expression simplified identically to the first two of the corresponding situation for E_0^*, but the third expression simplified even further than before. The third expression again dictates the stability of E_1^* when the chemother-

apy is inactive due to the first two expressions always being negative as previously discussed. Thus E_1^* will be stable if $a_0 < \frac{2a_0bd}{f}$ (or in a more simplified version $f < 2bd$) and the third eigenvalue expression then goes negative. Alternatively, E_1^* will be unstable if $a_0 > \frac{2a_0bd}{f}$ (or in a more simplified version $f > 2bd$) and the third eigenvalue expression then turns positive. However, because the conditional inequality for the third eigenvalue expression contains b, the reciprocal maximum tumor cell population level, i.e. a very small number, the other parameters will likely not have such magnitude so as to overcome the effects of b. Therefore the third eigenvalue expression is very likely to remain positive and cause E_1^* to become unstable when the drug therapy ceases. To verify these results, the same parameter values as have been used before along with $V_C = 0$ for the inactive drug therapy are substituted into the expressions.

$$\lambda_1 = -6.4000 \tag{3.78}$$

$$\lambda_2 = -0.3300 \tag{3.79}$$

$$\lambda_3 = 0.1168 \tag{3.80}$$

As suspected, the third eigenvalue resulted in a positive value and caused E_1^* to be unstable when the drug therapy is inactive. This again makes sense from a biological perspective as without the drug therapy to decrease the tumor cell population count further than what the native immune system can accomplish, there is nothing to keep the tumor cell population from increasing to the maximum stable population allowed. That tumor cell behavior corresponds with the equilibrium point E_1^* containing $T_1^* = 0$ being unstable.

3.2.3 Numerical Simulation

Three simulations are run to examine the two aforementioned scenarios where the drug therapy is either always active or always inactive as well as to simulate a realistic implementation of the drug therapy that sees the drugs alternating between being active and inactive for a time before remaining inactive for the remaining duration of the simulation.

Solving the chemotherapy model in MATLAB using ode45 with initial values of $T_0 = 3 \times 10^7$ for tumor cell population [24], $a_0 = 0.13$ for tumor cell growth [24], $b = 2.3 \times 9^{-10}$ for the reciprocal maximum tumor cell population level [24], $c_0 = 4.4 \times 10^{-9}$ as the competition coefficient between tumor cells and immune system cells [24], $d = 7.3 \times 10^6$ for the constant influx rate of immune system cells [24], $f = 0.33$ for the decay rate of immune cells [24], $V_C = 1$ for the chemotherapy influx rate [24], $p = 6.4$ for the chemotherapy decay rate [24], $M_T = 0.9$ for the tumor cell kill rate by the chemotherapy [24], and $M_L = 0.6$ for the immune cell kill rate by the chemotherapy [24], the first two graphs represent the simulations where the drug therapy is always active ($V_C = 1$) and then always inactive ($V_C = 0$), respectively. See Table A.1 for additional information regarding the model's initial values and parameter values.

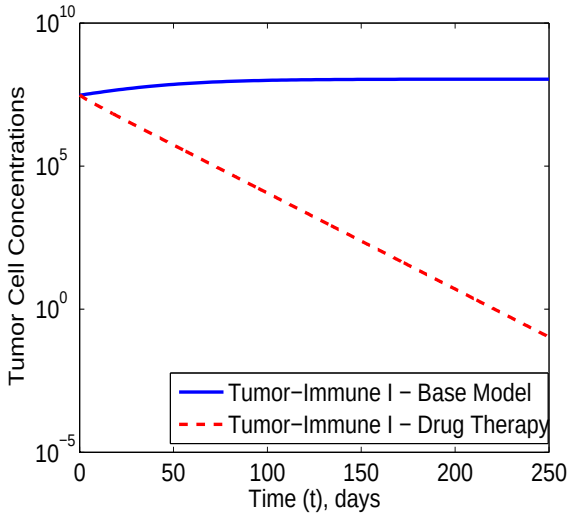

Figure 3.5: Tumor-Immune I - Drug Therapy Always Active

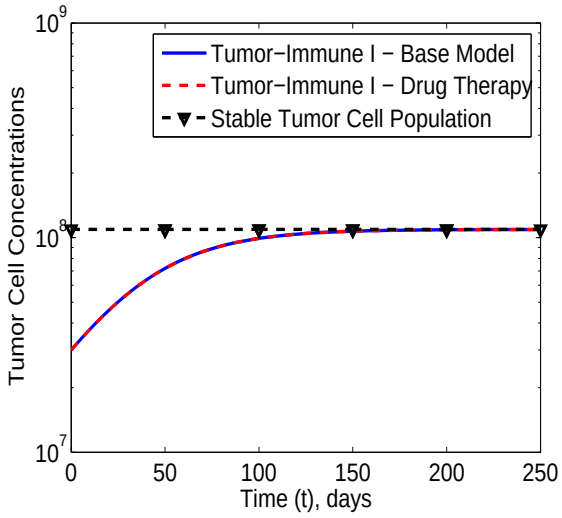

Figure 3.6: Tumor-Immune I - Drug Therapy Always Inactive

With the drug therapy always on, the tumor cells decrease linearly towards $T_1^* = 0$, confirming E_0^* as unstable and E_1^* as stable. When the drug therapy is always inactive, the tumor cell population grows identically to the Tumor-Immune I - Base Model and increases to $T_0^* = \frac{a_0 f - c_0 d}{a_0 b f} = 1.0925 \times 10^8$, thus confirming E_0^* as stable and E_1^* as unstable. The next simulation demonstrates a more likely implementation of the drug therapy instead of always being either active or inactive for the entire simulation.

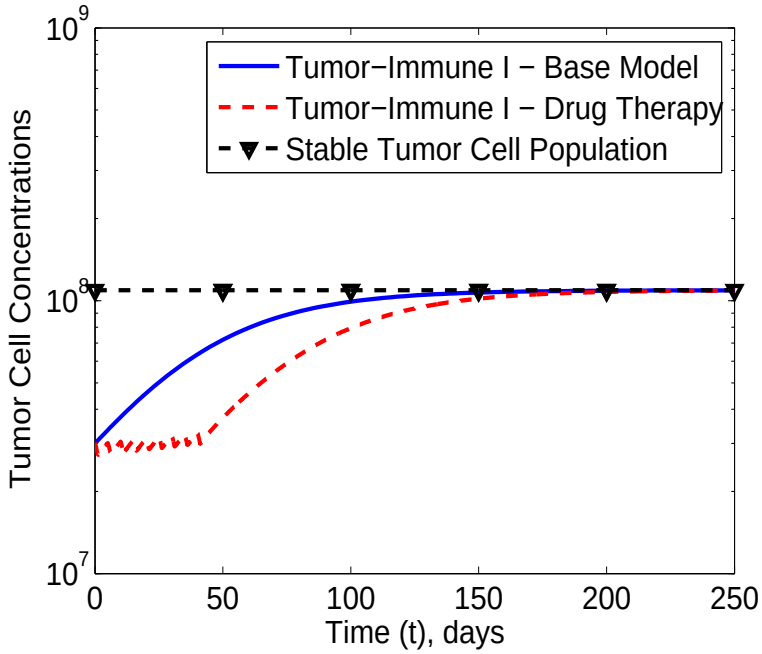

Figure 3.7: Tumor-Immune I - Drug Therapy

It is easy to identify when the chemotherapy is active in the model (the first portion of the model up to approximately day 40) versus when the chemotherapy is inactive (the remainder of the model). The oscillations during the active stage of drug therapy are due to the treatment going through a cycle of being active for one day and then inactive for the next four days. This cycle repeats a total of nine times, thus seeing the patient receive the last dose of drug therapy on day 40. Because the drug therapy is eventually inactive for the remainder of the simulation, the tumor cells do continue to multiply and grow towards the E_0^* equilibrium point since a prior model has shown the innate immune system not capable of sufficiently suppressing tumor growth on its own. While the method used in this model is successful in delaying the eventual growth of the tumor, it, too, is not sufficient in keeping the tumor cell

population at low levels, thus motivating the need for a slightly more complex model introduced in the next chapter.

CHAPTER 4

TUMOR-IMMUNE II

4.1 Base Model

4.1.1 Motivating the Model

The following model increases the complexity by adding a third substance into the model before any external terms, i.e. chemotherapy or immunotherapy, are interjected. This third substance, $IL-2$, aids in increasing the native immune system response to the tumor site by providing extra stiumulation to the influx of CTL immune cells. [24]

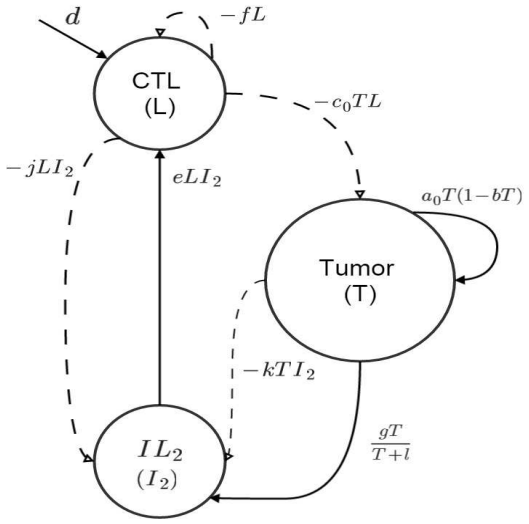

Figure 4.1: Tumor-Immune II - Base Model Interaction Diagram

With the additon of $IL-2$ to the model, the only changes from the Basic Tumor-Immune I model previously seen are the $IL-2$ equation as well a single

positive term in the immune cell equation modeling the increase in immune response as a result of the $IL-2$ presence. This immune cell response is increased by a term involving the variables L and I_2 for the CTL immune cells and $IL-2$ concentration, respectively, multiplied by an interaction coefficient, e. The $IL-2$ concentration is increased by the ratio of the tumor cell population and that same population plus a constant represented by l. This term is then multiplied by a coefficient g controlling the overall influx. The $IL-2$ concentration is then lessened by two interaction terms with the immune cells and tumor cells. These two terms contain respective interaction coefficients of j and k. No changes occur in the tumor cell equation, but, as expected, a change in the behavior of the cell population does occur as the model plays out from the greater concentration of immune cells at the tumor location.

$$\frac{dT}{dt} = a_0T(1-bT) - c_0TL \tag{4.1}$$
$$\frac{dL}{dt} = d + eLI_2 - fL \tag{4.2}$$
$$\frac{dI_2}{dt} = \frac{gT}{T+l} - jLI_2 - kTI_2 \tag{4.3}$$

4.1.2 Analysis of the Model

Finding equilibrium points of this three-equation model, the simultaneous Equations (4.1), (4.2), and (4.3) are first set equal to zero and solved for the variables T, L, and I_2.

$$\frac{dT}{dt} = a_0T(1-bT) - c_0TL = 0 \tag{4.4}$$
$$\frac{dL}{dt} = d + eLI_2 - fL = 0 \tag{4.5}$$
$$\frac{dI_2}{dt} = \frac{gT}{T+l} - jLI_2 - kTI_2 = 0 \tag{4.6}$$

Four potential equilibrium points result from solving the above system: two solutions are real, and the other two solution are complex. The complex solutions are not considered as applicable equilibrium points for this system. The first real solution is hand-calculated at the following:

$$T_0^* = 0 \tag{4.7}$$

$$L_0^* = \frac{d}{f} \tag{4.8}$$

$$I_{2_0}^* = 0 \tag{4.9}$$

The second real solution has a complex symbolic expression and is not explicitly expressed. Numerical expressions for this equilibrium point follows at a later point in the analysis.

Let E_0^* be the first equilibrium point where $T_0^* = 0$, $L_0^* = \frac{d}{f}$, and $I_{2_0}^* = 0$. To then find the stability of this equilibrium point, partial derivatives of each original model equation are found with respect to each model variable.

Let $T' = \frac{dT}{dt}$.

$$\frac{\partial T'}{\partial T} = a_0(1 - Tb) - Ta_0b - Lc_0 \tag{4.10}$$

$$\frac{\partial T'}{\partial L} = -Tc_0 \tag{4.11}$$

$$\frac{\partial T'}{\partial I_2} = 0 \tag{4.12}$$

Let $L' = \frac{dL}{dt}$.

$$\frac{\partial L'}{\partial T} = 0 \tag{4.13}$$
$$\frac{\partial L'}{\partial L} = I_2 e - f \tag{4.14}$$
$$\frac{\partial L'}{\partial I_2} = Le \tag{4.15}$$

Let $I_2' = \frac{dI_2}{dt}$.

$$\frac{\partial I_2'}{\partial T} = \frac{g}{T+l} - I_2 k - \frac{Tg}{(T+l)^2} \tag{4.16}$$
$$\frac{\partial I_2'}{\partial L} = -I_2 j \tag{4.17}$$
$$\frac{\partial I_2'}{\partial I_2} = -Lj - Tk \tag{4.18}$$

Let J be the Jacobian of the system. J_0 represents the Jacobian matrix evaluated at the first equilibrium point, E_0^*.

$$J = \begin{bmatrix} \frac{\partial T'}{\partial T} & \frac{\partial T'}{\partial L} & \frac{\partial T'}{\partial I_2} \\ \frac{\partial L'}{\partial T} & \frac{\partial L'}{\partial L} & \frac{\partial L'}{\partial I_2} \\ \frac{\partial I_2'}{\partial T} & \frac{\partial I_2'}{\partial L} & \frac{\partial I_2'}{\partial I_2} \end{bmatrix} \tag{4.19}$$

$$J = \begin{bmatrix} a_0(1-Tb) - Ta_0 b - Lc_0 & -Tc_0 & 0 \\ 0 & I_2 e - f & Le \\ \frac{g}{T+l} - I_2 k - \frac{Tg}{(T+l)^2} & -I_2 j & -Lj - Tk \end{bmatrix} \tag{4.20}$$

$$J_0 = \begin{bmatrix} a_0 - \frac{c_0 d}{f} & 0 & 0 \\ 0 & -f & \frac{de}{f} \\ \frac{g}{l} & 0 & -\frac{dj}{f} \end{bmatrix} \tag{4.21}$$

Having found J_0, the associated eigenvalues are calculated from the characteristic equation resulting from the determinant of J_0.

$$J_0 - \lambda I = \begin{bmatrix} a_0 - \frac{c_0 d}{f} - \lambda & 0 & 0 \\ 0 & -f - \lambda & \frac{de}{f} \\ \frac{g}{l} & 0 & -\frac{dj}{f} - \lambda \end{bmatrix} \tag{4.22}$$

$$det(J_0 - \lambda * I) = 0 \tag{4.23}$$

$$-\frac{(f+\lambda)(dj + f\lambda)(c_0 d - a_0 f + f\lambda)}{f^2} = 0 \tag{4.24}$$

$$\lambda_1 = -f \tag{4.25}$$

$$\lambda_2 = -\frac{dj}{f} \tag{4.26}$$

$$\lambda_3 = \frac{a_0 f - c_0 d}{f} \tag{4.27}$$

$$= a_0 - \frac{c_0 d}{f} \tag{4.28}$$

The equilibrium point E_0^* will be stable when all three eigenvalues have negative real parts and then unstable when all three eigenvalues have real parts with mixed signs. λ_1 will always be negative because f represents the immune cell death rate and $f > 0$ for the entire model. λ_2 will always be negative as well because d represents the immune cell induction rate, j represents the rate of consumption of $IL-2$ by the CTL immune cells, and f again represents the immune cell death rate. All three

parameters are always positive in this model ($d, j, f > 0$). Thus the stability of E_0^* is determined by λ_3. The equilibrium point E_0^* will be stable when the tumor growth rate, a_0, is less than the product of the constant influx of immune cells, d, and the tumor-immune competition coefficient, c_0, divided by the immune cell decay rate, f. Alternatively, the E_0^* will be unstable when the tumor growth rate is greater than the product of the constant influx of immune cells and the tumor-immune competition term divided by the immune cell decay rate. This particular eigenvalue has appeared in previous model analyses, and as such the expectation is its behavior will match that seen before of being positive. E_0^* is then expected to be unstable. This result is verified in the numerical simulations below.

Looking at the second real equilibrium point, because its symbolic expression is complex, MATLAB is employed to evaluate the numerical expression of the second equilibrium point. Using the parameter values of $a_0 = 0.13$ [24], $b = 2.3 \times 10^{-10}$ [24], $c_0 = 4.4 \times 10^{-9}$ [24], $d = 7.3 \times 10^6$ [24], $e = 9.9 \times 10^{-9}$ [24], $f = 0.33$ [24], $g = 1.6 \times 10^7$ [24], $j = 3.3 \times 10^{-9}$ [24], $k = 1.8 \times 10^{-8}$ [24], and $l = 3 \times 10^6$ [24] MATLAB arrives at the following numerical result for the second equilibrium point. See Table A.1 for additional information regarding the model's initial values and parameter values.

$$T_1^* = 1.6657 \times 10^5 \tag{4.29}$$

$$L_1^* = 2.9534 \times 10^7 \tag{4.30}$$

$$I_{2_1}^* = 8.3665 \times 10^6 \tag{4.31}$$

Thus let E_1^* be the second equilibrium point containing $T_1^* = 1.6657 \times 10^5$, $L_1^* = 2.9534 \times 10^7$, and $I_{2_1}^* = 8.3665 \times 10^6$. Finding the eigenvalues associated

with this equilibrium point follows the same process as before but differs in that the expressions will not be symbolic but rather will match the numerical nature of the equilibrium point values above. Using the same Jacobian matrix, J, as before, the numerical values of E_1^* are substituted into J to create J_1. Finding the determinant of J_1 to then solve the resulting characteristic equation yields the following numerical eigenvalues from MATLAB:

$$\lambda_1 = -0.2172 \tag{4.32}$$

$$\lambda_2 = -0.0652 + 0.0181\imath \tag{4.33}$$

$$\lambda_3 = -0.0652 - 0.0181\imath \tag{4.34}$$

Because all three eigenvalues have negative real parts, the second equilibrium point E_1^* is determined to be stable. The following numerical simulation will confirm this stability when using the respective initial values for model parameters and cell populations.

4.1.3 Numerical Simulation

Using the parameter values of $a_0 = 0.13$ for tumor cell growth [24], $b = 2.3 \times 10^{-10}$ for inverse tumor cell limiting population [24], $c_0 = 4.4 \times 10^{-9}$ as the competition coefficient between tumor cells and immune system cells [24], $d = 7.3 \times 10^6$ for the constant influx rate of immune system cells [24], $e = 9.9 \times 10^{-9}$ for the immune cell proliferation rate induced by $IL-2$ [24], $f = 0.33$ for the decay rate of immune cells [24], $g = 1.6 \times 10^7$ for the rate of antigen introduction [24], $j = 3.3 \times 10^{-9}$ for rate of consumption of $IL-2$ by the immune cells [24], $k = 1.8 \times 10^{-8}$ for the

rate of inactivation of $IL-2$ molecules by way of interacting with tumor cells [24], $l = 3 \times 10^6$ for the half-saturation constant [24], and the initial tumor population of $T_0 = 3 \times 10^7$, initial immune cell population of $L_0 = 2.3 \times 10^{-9}$, and initial $IL-2$ molecule concentration of $I_{20} = 2.4 \times 10^7$, MATLAB produces the following simulation. See Table A.1 for additional information regarding the model's initial values and parameter values.

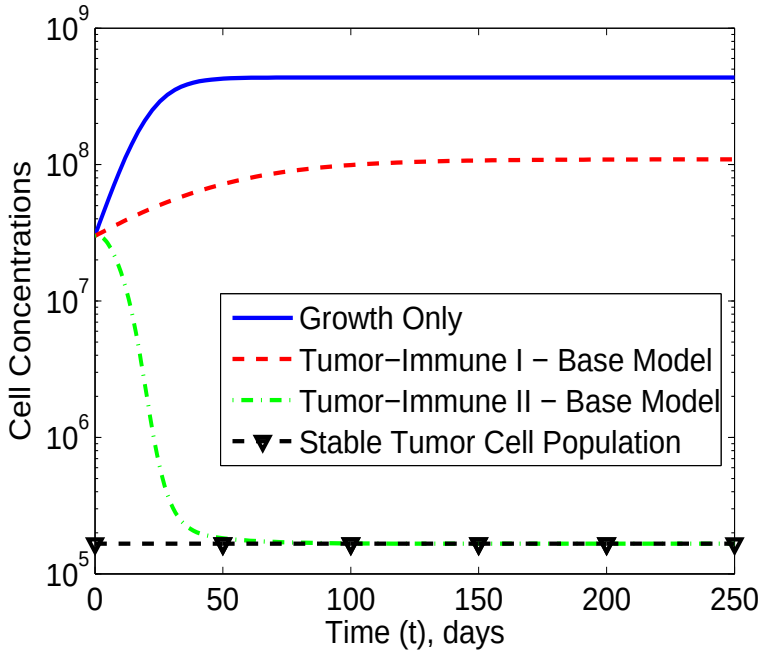

Figure 4.2: Tumor-Immune II - Base Model

The observed numerical results match that which is expected from the model analysis. The first equilibrium point, E_0^* is indeed unstable in the simulation as confirmed by substituting the appropriate parameters define above into the expressions for $\lambda_1, \lambda_2,$ and λ_3 of E_0^*.

$$\lambda_1 = -0.33 \tag{4.35}$$

$$\lambda_2 = -0.73 \tag{4.36}$$

$$\lambda_3 = 0.33 \tag{4.37}$$

λ_1 and λ_2 are negative as projected in the analysis, and λ_3 is positive and thus makes E_0^* unstable as suggested by the tumor cell population behavior in the previous simulation. E_1^* is also confirmed to be stable as previosly indicated by the numerical results of its eigenvalues. The next simulation will further test the stability analysis of the equilibrium points by instead increasing the immune cell induction rate parameter, d, from 7.3×10^6 to 7.3×10^7 and keeping all other parameters and initial values the same. This simulation should realize different behavior in the tumor cell population.

The tumor cell population in Figure (4.3) decreases to a minimum level with the changing of the single parameter. This simulation stops once the tumor cell population reaches the minimum level around day 25 and confirms the switching of stability of both equilibrium points, E_0^* and E_1^*, to be stable and unstable, respectively.

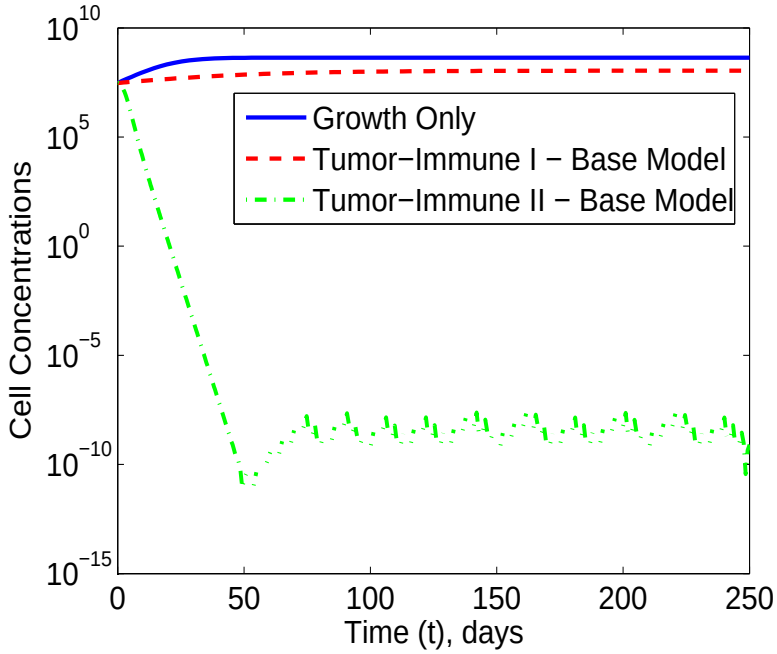

Figure 4.3: Tumor-Immune II - Base Model

4.2 Drug Therapy

4.2.1 Motivating the Model

The next iteration in this class of model builds upon the previous one by taking into account the effects of chemotherapy. $IL-2$, however, is not directly affected by the drug therapy unlike the tumor and immune cells.

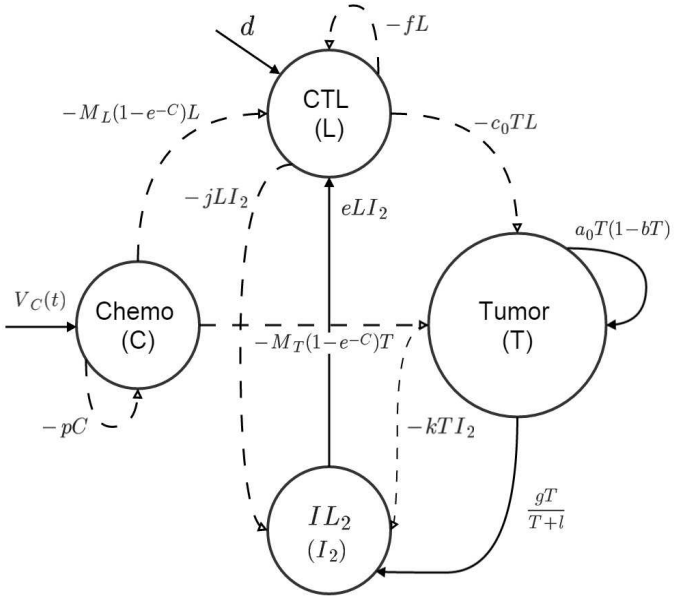

Figure 4.4: Tumor-Immune II - Drug Therapy Interaction Diagram

Just as in a prior model class and type, only the tumor cells and immune cells react to the presence of the chemotherapy. The drugs have the same time-dependant induction rate and decay rate as before, and the tumor cell kill rate and immune cell kill rate is identical to what was previously seen as well. Despite no change in the chemotherapy's immune cell kill rate, this model should prove more effective than even the chemotherapy model from the Tumor-Immune I drug therapy model due to the effects of $IL-2$ bringing in more immune cells at the onset.

$$\frac{dT}{dt} = a_0T(1-bT) - c_0TL - M_T(1-e^{-C})T \tag{4.38}$$

$$\frac{dL}{dt} = d + eLI_2 - fL - M_L(1-e^{-C})L \tag{4.39}$$

$$\frac{dC}{dt} = V_C(t) - pC \tag{4.40}$$

$$\frac{dI_2}{dt} = \frac{gT}{T+l} - jLI_2 - kTI_2 \tag{4.41}$$

4.2.2 Analysis of the Model

Finding equilibrium points of this four-equation model, the simultaneous Equations (4.38), (4.39), (4.40), and (4.41) are first set equal to zero and solved for the variables T, L, C, and I_2.

$$\frac{dT}{dt} = a_0T(1 - bT) - c_0TL - M_T(1 - e^{-C})T = 0 \tag{4.42}$$

$$\frac{dL}{dt} = d + eLI_2 - fL - M_L(1 - e^{-C})L = 0 \tag{4.43}$$

$$\frac{dC}{dt} = V_C(t) - pC = 0 \tag{4.44}$$

$$\frac{dI_2}{dt} = \frac{gT}{T + l} - jLI_2 - kTI_2 = 0 \tag{4.45}$$

In finding the equilibrium points of this model, one symbolic equilibrium point expression is found and one numerical equilibrium point is found by substituting in the applicable parameter values of the model [24]. Two additional numerical equilibrium points are discovered but are complex valued. As such those two equilibrium points are discarded as not being applicable. The first equilibrium point, E_0^*, is comprised of the following points:

$$T_0^* = 0 \tag{4.46}$$

$$L_0^* = \frac{d}{M_L(1 - \mathrm{e}^{-\frac{V_C}{p}}) + f} \tag{4.47}$$

$$C_0^* = \frac{V_C}{p} \tag{4.48}$$

$$I_{20}^* = 0 \tag{4.49}$$

The second equilibrium point, E_1^*, is comprised of the following points:

$$T_1^* = 1.6657 \times 10^5 \tag{4.50}$$

$$L_1^* = 2.9534 \times 10^7 \tag{4.51}$$

$$C_1^* = 8.3665 \times 10^6 \tag{4.52}$$

$$I_{21}^* = 0 \tag{4.53}$$

To establish the stability of these two equilibrium points, the partial differential equations of each original model equation are calculated with respect to each model variable, T, L, C, and I_2. The partial differential equations are then used to form the Jacobian matrix, J, of the system.

Let $T' = \frac{dT}{dt}$.

$$\frac{\partial T'}{\partial T} = M_T(\mathrm{e}^{-C} - 1) - Lc_0 - a_0(Tb - 1) - Ta_0b \tag{4.54}$$
$$\frac{\partial T'}{\partial L} = -Tc_0 \tag{4.55}$$
$$\frac{\partial T'}{\partial C} = -\frac{M_T T}{\mathrm{e}^C} \tag{4.56}$$
$$\frac{\partial T'}{\partial I_2} = 0 \tag{4.57}$$

Let $L' = \frac{dL}{dt}$.

$$\frac{\partial L'}{\partial T} = 0 \tag{4.58}$$
$$\frac{\partial L'}{\partial L} = I_2 e - f + M_L(\mathrm{e}^{-C} - 1) \tag{4.59}$$
$$\frac{\partial L'}{\partial C} = -\frac{M_L L}{\mathrm{e}^C} \tag{4.60}$$
$$\frac{\partial L'}{\partial I_2} = Le \tag{4.61}$$

Let $C' = \frac{dC}{dt}$.

$$\frac{\partial C'}{\partial T} = 0 \tag{4.62}$$
$$\frac{\partial C'}{\partial L} = 0 \tag{4.63}$$
$$\frac{\partial C'}{\partial C} = -p \tag{4.64}$$
$$\frac{\partial C'}{\partial I_2} = 0 \tag{4.65}$$

Let $I_2' = \frac{dI_2}{dt}$;

$$\frac{\partial I_2'}{\partial T} = \frac{g}{T+l} - I_2 k - \frac{Tg}{(T+l)^2} \tag{4.66}$$

$$\frac{\partial I_2'}{\partial L} = -I_2 j \tag{4.67}$$

$$\frac{\partial I_2'}{\partial C} = 0 \tag{4.68}$$

$$\frac{\partial I_2'}{\partial I_2} = -Lj - Tk \tag{4.69}$$

Let J be the Jacobian of the system. J_0 represents the Jacobian matrix evaluated at the first equilibrium point, E_0^*.

$$J = \begin{bmatrix} \frac{\partial T'}{\partial T} & \frac{\partial T'}{\partial L} & \frac{\partial T'}{\partial C} & \frac{\partial T'}{\partial I_2} \\ \frac{\partial L'}{\partial T} & \frac{\partial L'}{\partial L} & \frac{\partial L'}{\partial C} & \frac{\partial L'}{\partial I_2} \\ \frac{\partial C'}{\partial T} & \frac{\partial C'}{\partial L} & \frac{\partial C'}{\partial C} & \frac{\partial C'}{\partial I_2} \\ \frac{\partial I_2'}{\partial T} & \frac{\partial I_2'}{\partial L} & \frac{\partial I_2'}{\partial C} & \frac{\partial I_2'}{\partial I_2} \end{bmatrix} \tag{4.70}$$

Due to the length and complexity of the expressions, both J and J_0 with the respective substituted expressions and values are omitted.

Finding the eigenvalues of E_0^* requires the determinant of J_0 and then solving the resulting characteristic equation for λ. MATLAB produces the resulting eigenvalues:

$$\lambda_1 = -p \tag{4.71}$$

$$\lambda_2 = M_L(\mathrm{e}^{-\frac{V_C}{p}} - 1) - f \tag{4.72}$$

$$\lambda_3 = -\frac{dj}{M_L + f - M_L\mathrm{e}^{-\frac{V_C}{p}}} \tag{4.73}$$

$$\lambda_4 = \{\text{symbolic expression is of excessive length}\} \tag{4.74}$$

Most of the eigenvalues have simple symbolic expressions, but λ_4 has a lengthy symbolic expression and as such is omitted. Similar to before, due to the presence of the V_C term being active and then inactive at varying times during the model implementation, there are two situations to analyze. The first situation finds the drug therapy active, i.e. V_C is a positive constant. When this occurs, the λ_1 remains negative due to p being the chemotherapy decay rate and $p > 0$ for the entire model. λ_2 has a sign dependent on the difference between the remaining portion of the difference between the two M_L, immune cell kill rate by chemotherapy, and f, the immune cell death rate. This is due to the $\mathrm{e}^{-\frac{V_C}{p}}$ term being a multiplier on M_L of at least 1. The sign of λ_3 is dependent on the sum between the difference of M_L and itself with a multiplier dictated by the $\mathrm{e}^{-\frac{V_C}{p}}$ term and then f again. The sign of this denominator in λ_3 dictates the sign as the numerator will always remain negative with both d, immune cell induction rate, and j, rate of consumption of $IL-2$ by immune cells, always being positive in this model. The sign of λ_4 is evaluated numerically with its complex symbolic expression. Using the values of the aforementioned parameters, the following are the numerical values of the four eigenvalues when the drug therapy is active, i.e. $V_C = 1$:

$$\lambda_1 = -6.4000 \tag{4.75}$$

$$\lambda_2 = -0.0578 \tag{4.76}$$

$$\lambda_3 = -0.4168 \tag{4.77}$$

$$\lambda_4 = -0.0773 \tag{4.78}$$

With all four eigenvalues negative, E_0^* is considered stable when the drug therapy is active. The next situation dictates the stability of E_0^* when the drug therapy is inactive ($V_C = 0$). The matrices J and J_0 remain the same, but with the simplicity offered by $V_C = 0$ the symbolic expressions for the four eigenvalues are substantially less complex:

$$\lambda_1 = -p \tag{4.79}$$

$$\lambda_2 = -f \tag{4.80}$$

$$\lambda_3 = -\frac{dj}{f} \tag{4.81}$$

$$\lambda_4 = \frac{a_0 f - c_0 d}{f} \tag{4.82}$$

$$= a_0 - \frac{c_0 d}{f} \tag{4.83}$$

λ_1, λ_2, and λ_3 have negative signs since all of the parameters in those expressions, d, f, j, and p stay positive the entire model. The stability of E_0^* when the drug therapy is inactive is thus decided by λ_4. Fortunately this exact expression is recurring in the various analyses performed, and it has expected behavior of being positive.

Using values of the aforementioned parameters, the following are the numerical values of the four eigenvalues when the drug therapy is inactive:

$$\lambda_1 = -6.4000 \tag{4.84}$$

$$\lambda_2 = -0.3300 \tag{4.85}$$

$$\lambda_3 = -0.0730 \tag{4.86}$$

$$\lambda_4 = 0.0327 \tag{4.87}$$

As expexted the sign of λ_4 is positive and thus makes E_0^* unstable when the drug therapy is inactive. The numerical results at the end of this section confirm the results of the analysis. Turning to the second equilibrium point, E_1^*, the same Jacobian matrix, J, is used to first substituate the values of E_1^* to then find J_1. The determinant of J_1 is next computed, and the subsequent characteristic equation is solved to produce the following eigenvalues:

$$\lambda_1 = -6.4000 \tag{4.88}$$

$$\lambda_2 = -0.1020 \tag{4.89}$$

$$\lambda_3 = -0.8757 \tag{4.90}$$

$$\lambda_4 = -0.9528 \tag{4.91}$$

With all four eigenvalues having negative real parts, E_1^* is established as stable. Because $V_C = 0$ when E_1^* is computed due to being inactive for most of the model

duration, it is now known for E_1^* to be stable when the chemotherapy is inactive. The following numerical simulation will confirm the results of the analysis for E_1^*.

4.2.3 Numerical Simulation

Three simulations are run to examine the two aforementioned scenarios where the drug therapy is either always active or always inactive as well as to simulate a realistic implementation of the drug therapy that sees the drugs alternating between being active and inactive before remaining inactive for the remaining duration of the simulation. The drug therapy is active once every five days for a total of nine doses.

Using the parameter values of $a_0 = 0.13$ [24], $b = 2.3\times10^{-10}$ [24], $c_0 = 4.4\times10^{-9}$ [24], $d = 7.3 \times 10^6$ [24], $e = 9.9 \times 10^{-9}$ [24], $f = 0.33$ [24], $g = 1.6 \times 10^7$ [24], $j = 3.3 \times 10^{-9}$ [24], $k = 1.8 \times 10^{-8}$ [24], $l = 3 \times 10^6$ [24], $p = 6.4$ [24], $M_T = 0.9$ [24], and $M_L = 0.6$ [24], and the initial tumor population of $T_0 = 3 \times 10^7$ [24], initial immune cell population of $L_0 = 2.3 \times 10^{-9}$ [24], and initial $IL-2$ molecule concentration of $I_{20} = 2.4 \times 10^7$ [24], the first two graphs represent the simulations where the drug therapy is always active $V_C = 1$ and then always inactive $V_C = 0$, respectively. See Table A.1 for additional information regarding the model's initial values and parameter values.

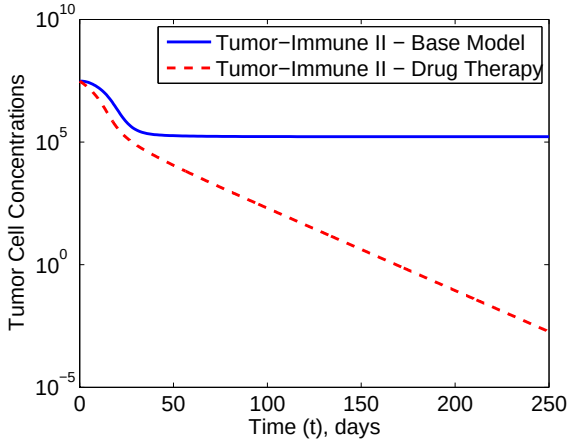

Figure 4.5: Tumor-Immune II - Drug Therapy - Always Active

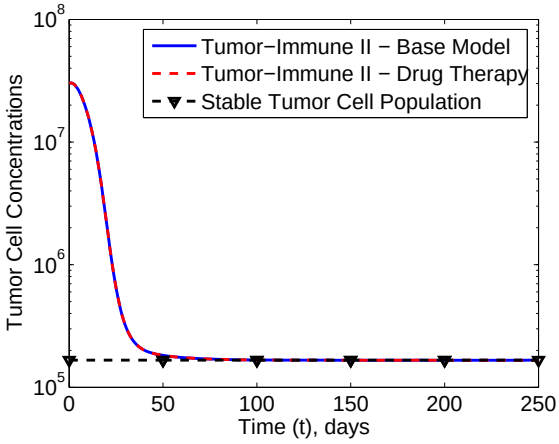

Figure 4.6: Tumor-Immune II - Drug Therapy - Always Inactive

With the drug therapy always on, the tumor cells decrease linearly towards $T_0^* = 0$, confirming E_0^* stable. The tumor cell levels reach sufficiently low levels around day 170, thus halting the simulation. When the drug therapy is always inactive, the tumor cell population identically follows the population levels of the Tumor-Immune II - Base Model and settles at $T = \frac{a_0 f - c_0 d}{a_0 b d} = 1.6657 \times 10^5$, thus confirming E_0^* as unstable and E_1^* as stable at this point in the model. The next simulation demonstrates a more likely implementation of the drug therapy as the chemotherapy is administered in a time-dependent manner.

Just as in the Tumor-Immune I - Drug Therapy model, it is easy to identify in Figure (4.7) when the chemotherapy is active as opposed to when the chemotherapy is inactive. The oscillations during the active stage occur because the treatment is going through a cycle of being active for one day and then inactive for the next four days. This cycle repeats a total of nine times, thus seeing the patient receive the last dose of drug therapy on day 40. Because the drug therapy is eventually inactive for the remainder of the simulation, the tumor cells do continue to multiply and grow

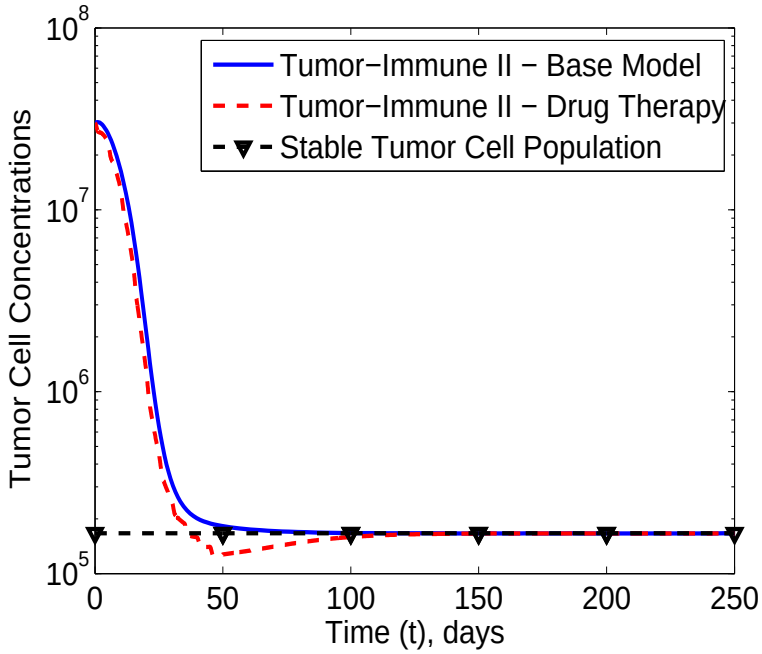

Figure 4.7: Tumor-Immune II - Drug Therapy

towards a stable population level. While the method used in this model is much more successful in initially combating the tumor cells and even shrinking the tumor to a level unseen with the prior models, it still cannot keep decreasing the tumor cell population to continually lower levels, thus motivating the investigation into further models.

4.3 Immunotherapy

4.3.1 Motivating the Model

This particular model is incredibly similar in motivation to the immediately preceeding model in that the base model of this class is modified only by adding in an external stimulus. Instead of chemotherapy, however, this model implements immunotherapy to boost the $IL-2$ concentration near the tumor's location and thus increase the innate immune response.

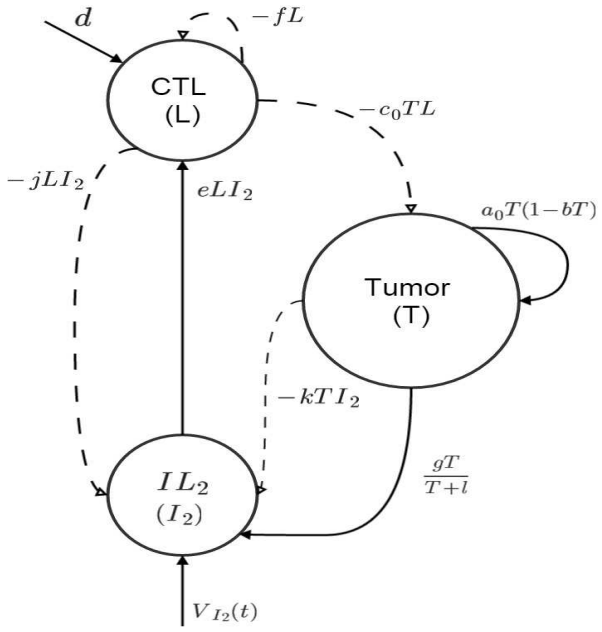

Figure 4.8: Tumor-Immune II - Immunotherapy Interaction Diagram

A time-dependent function simulates an induction rate of the boosted $IL-2$ concentration to accompany the naturally occuring influx of $IL-2$. The decay rate and interaction coefficient with the immune cell variable, L, remain the same. This model aims to be more efficient at combating the tumor with increased immune cell populations as a result of increased $IL-2$ concentrations at the tumor location.

$$\frac{dT}{dt} = a_0T(1-bT) - c_0TL \tag{4.92}$$

$$\frac{dL}{dt} = d + eLI_2 - fL \tag{4.93}$$

$$\frac{dI_2}{dt} = V_{I_2}(t) + \frac{gT}{T+l} - jLI_2 - kTI_2 \tag{4.94}$$

4.3.2 Analysis of the Model

Finding equilibrium points of this three-equation model, the simultaneous Equations (4.92), (4.93), and (4.94) are first set equal to zero and solved for the variables T, L, and I_2.

$$\frac{dT}{dt} = a_0 T(1 - bT) - c_0 TL = 0 \tag{4.95}$$

$$\frac{dL}{dt} = d + eLI_2 - fL = 0 \tag{4.96}$$

$$\frac{dI_2}{dt} = V_{I_2}(t) + \frac{gT}{T + l} - jLI_2 - kTI_2 = 0 \tag{4.97}$$

When performing calculations to find the equilibrium points of this model, one symbolic expression is found, one real numerical expression, and two complex numerical expressions. As before, the two complex expressions are discarded for not being applicable in this model. The symbolic expression is fully analyzed, and the numerical expression is numerically analyzed as much as possible. Let E_0^* represent the first equilibrium point with the following values:

$$T_0^* = 0 \tag{4.98}$$

$$L_0^* = \frac{V_{I_2} e + dj}{fj} \tag{4.99}$$

$$I_{2_0}^* = \frac{V_{I_2} f}{V_{I_2} e + dj} \tag{4.100}$$

Using the appropriate model parameters of $a_0 = 0.13$ [24], $b = 2.3 \times 10^{-10}$ [24], $c_0 = 4.4 \times 10^{-9}$ [24], $d = 7.3 \times 10^6$ [24], $e = 9.9 \times 10^{-9}$ [24], $f = 0.33$ [24], $g = 1.6 \times 10^7$

[24], $j = 3.3 \times 10^{-9}$ [24], $k = 1.8 \times 10^{-8}$ [24], $l = 3 \times 10^{6}$ [24], MATLAB arrives at the following for the numerical representation of the second equilibrium. Let E_1^* represent the second equilibrium point with the following values. See Table A.1 for additional information regarding the model's initial values and parameter values.

$$T_1^* = 1.6657 \times 10^5 \tag{4.101}$$

$$L_1^* = 2.9534 \times 10^7 \tag{4.102}$$

$$I_{2_1}^* = 8.3665 \times 10^6 \tag{4.103}$$

Adhering to the usual process previously established in prior sections, finding the stability of E_0^* first requires the partial derivatives of each model equation taken with respect to the model variables T, L, and I_2.

Let $T' = \frac{dT}{dt}$.

$$\frac{\partial T'}{\partial T} = -Lc_0 - a_0(Tb - 1) - Ta_0b \tag{4.104}$$

$$\frac{\partial T'}{\partial L} = -Tc_0 \tag{4.105}$$

$$\frac{\partial T'}{\partial I_2} = 0 \tag{4.106}$$

Let $L' = \frac{dL}{dt}$.

$$\frac{\partial L'}{\partial T} = 0 \tag{4.107}$$
$$\frac{\partial L'}{\partial L} = I_2 e - f \tag{4.108}$$
$$\frac{\partial L'}{\partial I_2} = Le \tag{4.109}$$

Let $I_2' = \frac{dI_2}{dt}$;

$$\frac{\partial I_2'}{\partial T} = \frac{g}{T+l} - I_2 k - \frac{Tg}{(T+l)^2} \tag{4.110}$$
$$\frac{\partial I_2'}{\partial L} = -I_2 j \tag{4.111}$$
$$\frac{\partial I_2'}{\partial I_2} = -Lj - Tk \tag{4.112}$$

Let J be the Jacobian of the system. J_0 represents the Jacobian matrix evaluated at the first equilibrium point, E_0^*.

$$J = \begin{bmatrix} \frac{\partial T'}{\partial T} & \frac{\partial T'}{\partial L} & \frac{\partial T'}{\partial I_2} \\ \frac{\partial L'}{\partial T} & \frac{\partial L'}{\partial L} & \frac{\partial L'}{\partial I_2} \\ \frac{\partial I_2'}{\partial T} & \frac{\partial I_2'}{\partial L} & \frac{\partial I_2'}{\partial I_2} \end{bmatrix} \tag{4.113}$$

$$J = \begin{bmatrix} -Lc_0 - a_0(Tb-1) - Ta_0 b & -Tc_0 & 0 \\ 0 & I_2 e - f & Le \\ \frac{g}{T+l} - I_2 k - \frac{Tg}{(T+l)^2} & -I_2 j & -Lj - Tk \end{bmatrix} \tag{4.114}$$

$$J_0 = \begin{bmatrix} a_0 - \frac{c_0(V_{I_2} e + dj)}{fj} & 0 & 0 \\ 0 & \frac{V_{I_2} ef}{V_{I_2} e + dj} - f & \frac{e(V_{I_2} e + dj}{fj} \\ \frac{g}{l} - \frac{V_{I_2} fk}{V_{I_2} e + dj} & -\frac{V_{I_2} fj}{V_{I_2} e + dj} & -\frac{V_{I_2} e + dj}{f} \end{bmatrix} \tag{4.115}$$

Finding the eigenvalues of E_0^* requires the determinant of J_0 and then solving the resulting characteristic equation for λ. Unfortunately the symbolic expressions for each respective eigenvalue become very lengthy and thus prevent further symbolic analysis. Numerical results, however, are still attainable and indicate the stability of the first equilibrium point, E_0^*. The parameter values of $a_0 = 0.13$ [24], $b = 2.3 \times 10^{-10}$ [24], $c_0 = 4.4 \times 10^{-9}$ [24], $d = 7.3 \times 10^6$ [24], $e = 9.9 \times 10^{-9}$ [24], $f = 0.33$ [24], $g = 1.6 \times 10^7$ [24], $j = 3.3 \times 10^{-9}$ [24], $k = 1.8 \times 10^{-8}$ [24], $l = 3 \times 10^6$ [24], and $V_{I_2} = 10 \times 10^6$ [24] are substituted into the eigenvalue expressions via MATLAB and produce the following numerical results of the eigenvalues. See Table A.1 for additional information regarding the model's initial values and parameter values.

$$\lambda_1 = -0.3673 \tag{4.116}$$

$$\lambda_2 = -0.2188 + 0.2743\imath \tag{4.117}$$

$$\lambda_3 = -0.2188 - 0.2743\imath \tag{4.118}$$

Each calculated eigenvalue results in having negative real parts, thus indicating E_0^* containing $T_0^* = 0$ is stable when the immunotherapy is active. This is a logical conclusion when the immunotherapy is an effective treatment. Otherwise the tumor cells would continue to trend towards a substantially large non-zero level of population rendering the immunotherapy useless. The above results, however, are only when the immunotherapy is active. Performing the same calculations with the same parameter

set as before via MATLAB when the immunotherapy is inactive, i.e. $V_{I_2} = 0$, yields the next set of eigenvalues:

$$\lambda_1 = -0.3300 \tag{4.119}$$

$$\lambda_2 = 0.0327 \tag{4.120}$$

$$\lambda_3 = -0.0730 \tag{4.121}$$

Having mixed signs for each respective real part of the eigenvalues makes E_0^* unstable when the immunotherapy is inactive, confirming the logical notion of continued tumor existence when the immunotherapy treatment ceases. The stability or instability of E_0^* suggested by the above analyses is confirmed in numerical simulations at the end of the current section.

Revisiting the numerical representation of the second equilibrium point, E_1^*, the same Jacobian matrix is used to begin the process of establishing the stability of E_1^*. Substituing the numerical values of E_1^* and appropriate parameters as previously noted into J creates the matrix J_1 of which the determinant is taken and characteristic equation solved to then find the respective eigenvalues.

$$\lambda_1 = -0.2171 \tag{4.122}$$

$$\lambda_2 = -0.0653 + 0.0175\imath \tag{4.123}$$

$$\lambda_3 = -0.0653 - 0.0175\imath \tag{4.124}$$

Because E_1^* is represented only by numerical values and not a symbolic representation, there are no variables, namely V_{I_2}, to modulate for further investigation of any changes in stability upon activation or inactivation of external treatments. Because the immunotherapy is only temporarily active, E_1^* is calculated with the treatment inactive, i.e. $V_{I_2} = 0$, and thus is classified as being stable by the above eigenvalues having all negative real parts. With $T_1^* = 1.6657 \times 10^5$ and the immunotherapy treatment inactive, the result of this stability analysis is expected and confirmed in the following numerical simulations.

4.3.3 Numerical Simulation

This model is highlighted by the inclusion of the external immunotherapy term, V_{I_2}, in the third model equation as previously listed. The first simulation below is when the immunotherapy treatment is active ($V_{I_2} = 10 \times 10^6$) for the entire duration of the model.

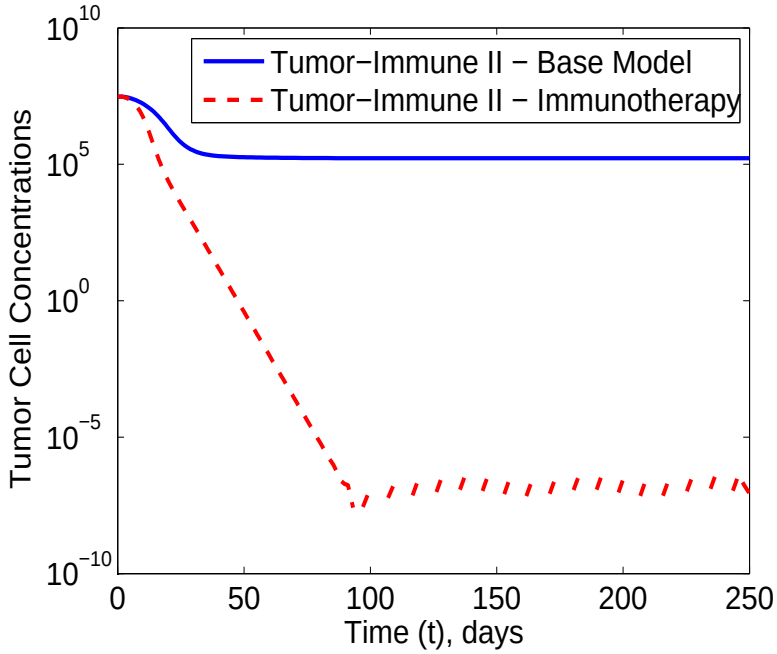

Figure 4.9: Tumor-Immune II - Immunotherapy Always Active

The simulation matches the results of the analysis in that the tumor cell population decreases uniformly to a minimum level and confirms the stable condition of E_0^* with the constant activation of the immunotherapy. Once the tumor cell levels are sufficiently low around day 50, the simulation halts. The next simulation runs the opposite condition, i.e. immunotherapy always inactive ($V_{I_2} = 0$).

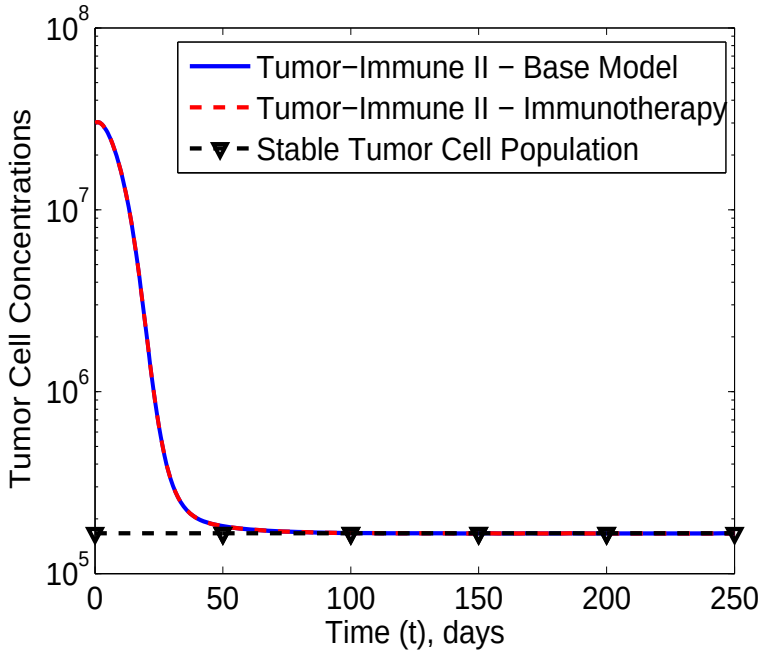

Figure 4.10: Tumor-Immune II - Immunotherapy Always Inactive

This second simulation again matches the results of the respective analysis in that the tumor cell population exactly matches the behavior of the tumor cell population in the Tumor-Immune II - Base Model and stabilizes at $T_1^* = 1.6657 \times 10^5$ thus confirming the stability of E_1^* and instability of E_0^* when the immunotherapy is inactive. The next simulation utilizes the proscribed administration of the immunotherapy treatment with a 10 MU/day dose with four days active per dose on a 10-day cycle. That is, the 10 MU/day dose is maintained for four days and then turns inactive to allow the therapy to decay at its own specified rate for the remaining six days of the cycle. There are four doses total before the immunotherapy stays inactive for the rest of the model time period.

The immunotherapy treatment proves to be substantially more effective than the chemotherapy treatment over the same initial timeframe. However, just as with

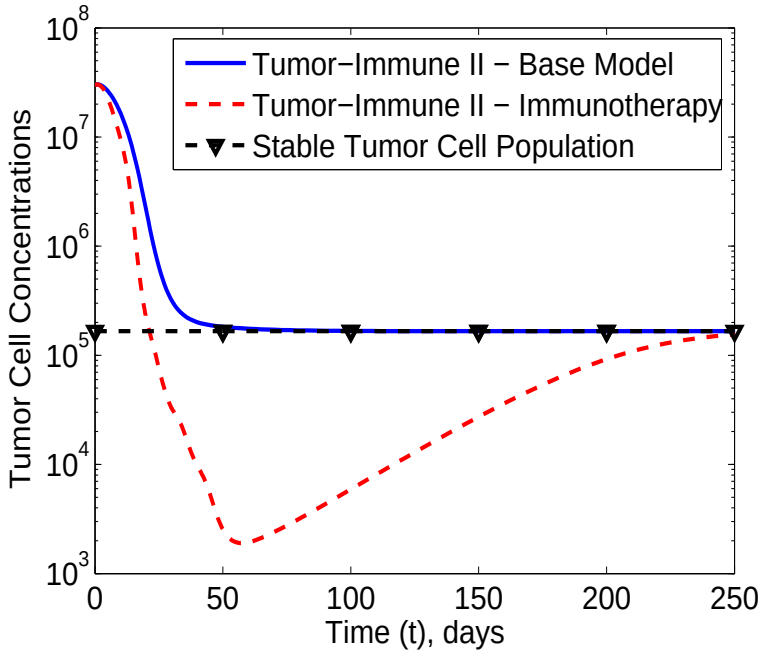

Figure 4.11: Tumor-Immune II - Immunotherapy

the drug therapy, once the immunotherapy turns inactive, the tumor cells do return to the stable state of the base model. The next model investigates the behavior of the tumor cell population when both treatments are combined concurrently.

4.4 Combined Drug Therapy and Immunotherapy

4.4.1 Motivating the Model

The final model of this class and of this discussion takes the Tumor-Immune II - Base Model and combines the efforts of both the chemotherapy and immunotherapy. Because both external stimuli are independent of each other, combining the two should ideally stack their respective abilities at tumor cell eradication.

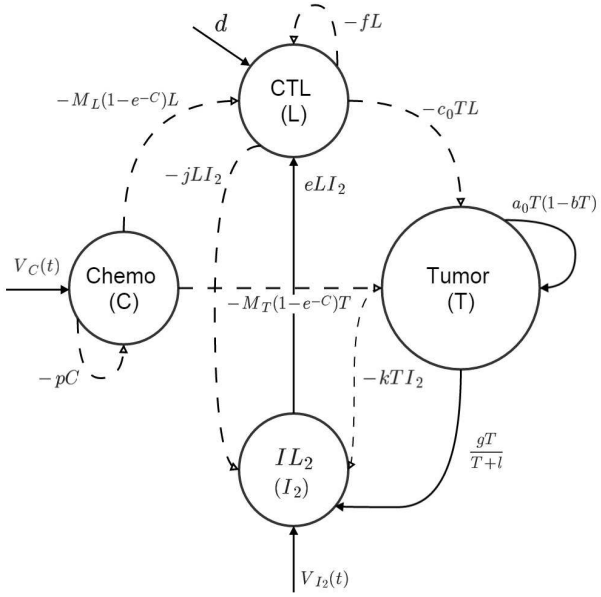

Figure 4.12: Tumor-Immune II - Drug Therapy and Immunotherapy Interaction Diagram

All of the respective parameters, functions, and coefficients related to the previous two models are identical in this aggregate model. Because neither the chemotherapy nor immunotherapy is directly affected by the other, this model successfully implements both simultaneously to investigate their combined effects on the tumor cells.

$$\frac{dT}{dt} = a_0T(1-bT) - c_0TL - M_T(1-e^{-C})T \tag{4.125}$$

$$\frac{dL}{dt} = d + eLI_2 - fL - M_L(1-e^{-C})L \tag{4.126}$$

$$\frac{dC}{dt} = V_C(t) - pC \tag{4.127}$$

$$\frac{dI_2}{dt} = V_{I_2}(t) + \frac{gT}{T+l} - jLI_2 - kTI_2 \tag{4.128}$$

4.4.2 Analysis of the Model

Finding equilibrium points of this four-equation model, the simultaneous Equations (4.125), (4.126), (4.127), and (4.128) are first set equal to zero and solved for the variables T, L, C, and I_2.

$$\frac{dT}{dt} = a_0T(1 - bT) - c_0TL - M_T(1 - e^{-C})T = 0 \tag{4.129}$$

$$\frac{dL}{dt} = d + eLI_2 - fL - M_L(1 - e^{-C})L = 0 \tag{4.130}$$

$$\frac{dC}{dt} = V_C(t) - pC = 0 \tag{4.131}$$

$$\frac{dI_2}{dt} = V_{I_2}(t) + \frac{gT}{T + l} - jLI_2 - kTI_2 = 0 \tag{4.132}$$

In calculating the equilibrium points of this model, one symbolic expression, one real numerical expression, and two complex numerical expressions are found. The numerical equilibrium points are calculated by substituting the appropriate parameter values [24] into the expressions. As before, the two complex expressions are discarded for not being applicable in this model. The symbolic expression is fully analyzed, and the numerical expression is numerically analyzed as much as possible. Let E_0^* represent the first equilibrium point with the following values:

$$T_0^* = 0 \tag{4.133}$$

$$L_0^* = \frac{dj + eV_{I_2}}{j(f + M_L(1 - \mathrm{e}^{-\frac{V_C}{p}}))} \tag{4.134}$$

$$C_0^* = \frac{V_C}{p} \tag{4.135}$$

$$I_{2_0}^* = \frac{V_{I_2}(f + M_L(1 - \mathrm{e}^{-\frac{V_C}{p}}))}{dj + eV_{I_2}} \tag{4.136}$$

The second equilibrium point, E_1^*, is comprised of the following points:

$$T_1^* = 1.6657 \times 10^5 \tag{4.137}$$

$$L_1^* = 2.9534 \times 10^7 \tag{4.138}$$

$$C_1^* = 8.3665 \times 10^6 \tag{4.139}$$

$$I_{2_1}^* = 0 \tag{4.140}$$

Establishing the stability of each equilibrium point first requires the partial derivatives of each model equation taken with respect to each model variable ($T, L, C,$ and I_2). The Jacobian matrix, J, is then formed from these partial derivative expressions.

Let $T' = \frac{dT}{dt}$.

$$\frac{\partial T'}{\partial T} = M_T(\mathrm{e}^{-C} - 1) - Lc_0 - a_0(Tb - 1) - Ta_0b \tag{4.141}$$

$$\frac{\partial T'}{\partial L} = -Tc_0 \tag{4.142}$$

$$\frac{\partial T'}{\partial C} = -\frac{M_T T}{\mathrm{e}^C} \tag{4.143}$$

$$\frac{\partial T'}{\partial I_2} = 0 \tag{4.144}$$

Let $L' = \frac{dL}{dt}$.

$$\frac{\partial L'}{\partial T} = 0 \tag{4.145}$$
$$\frac{\partial L'}{\partial L} = I_2 e - f + M_L(\mathrm{e}^{-C} - 1) \tag{4.146}$$
$$\frac{\partial L'}{\partial C} = -\frac{M_L L}{\mathrm{e}^C} \tag{4.147}$$
$$\frac{\partial L'}{\partial I_2} = Le \tag{4.148}$$

Let $C' = \frac{dC}{dt}$.

$$\frac{\partial C'}{\partial T} = 0 \tag{4.149}$$
$$\frac{\partial C'}{\partial L} = 0 \tag{4.150}$$
$$\frac{\partial C'}{\partial C} = -p \tag{4.151}$$
$$\frac{\partial C'}{\partial I_2} = 0 \tag{4.152}$$

Let $I_2' = \frac{dI_2}{dt}$;

$$\frac{\partial I_2'}{\partial T} = \frac{g}{T+l} - I_2 k - \frac{Tg}{(T+l)^2} \tag{4.153}$$
$$\frac{\partial I_2'}{\partial L} = -I_2 j \tag{4.154}$$
$$\frac{\partial I_2'}{\partial C} = 0 \tag{4.155}$$
$$\frac{\partial I_2'}{\partial I_2} = -Lj - Tk \tag{4.156}$$

Let J be the Jacobian of the system. Focusing on the first equilibrium point, J_0 represents the Jacobian matrix evaluated at the first equilibrium point, E_0^*.

$$J = \begin{bmatrix} \frac{\partial T'}{\partial T} & \frac{\partial T'}{\partial L} & \frac{\partial T'}{\partial C} & \frac{\partial T'}{\partial I_2} \\ \frac{\partial L'}{\partial T} & \frac{\partial L'}{\partial L} & \frac{\partial L'}{\partial C} & \frac{\partial L'}{\partial I_2} \\ \frac{\partial C'}{\partial T} & \frac{\partial C'}{\partial L} & \frac{\partial C'}{\partial C} & \frac{\partial C'}{\partial I_2} \\ \frac{\partial I_2'}{\partial T} & \frac{\partial I_2'}{\partial L} & \frac{\partial I_2'}{\partial C} & \frac{\partial I_2'}{\partial I_2} \end{bmatrix} \tag{4.157}$$

Due to the length of the expressions, both J and J_0 with the respective substituted expressions and values are omitted. Finding the eigenvalues of E_0^* requires the determinant of J_0 and then solving the resulting characteristic equation for λ. These expressions are similarly complex and lengthy and are thus omitted in their symbolic form. It should be noted, however, this system is also non-autonomous as all the previous ones containing either the time-dependent chemotherapy or immunotherapy term. As such, multiple computations of eigenvalues are necessitated to investigate the stability of E_0^* when either or both of the drug therapy and immunotherapy parameters (V_C and V_{I_2}, respectively) are either active or inactive. Using the remainder of the applicable parameter set [24] and setting both chemotherapy and immunotherapy treatments as active ($V_C = 1$ and $V_{I_2} = 10 \times 10^6$ [24]), MATLAB produces the resulting eigenvalues:

$$\lambda_1 = -6.4000 \tag{4.158}$$

$$\lambda_2 = -0.3940 \tag{4.159}$$

$$\lambda_3 = -0.1884 + 0.2959\imath \tag{4.160}$$

$$\lambda_4 = -0.1884 - 0.2959\imath \tag{4.161}$$

With all four eigenvalues having negative real parts, E_0^* containing $T_0^* = 0$ is determined to be stable when both the drug therapy and immunotherapy terms are active. Repeating the eigenvalue calculations but with the drug therapy active ($V_C = 1$) and immunotherapy inactive ($V_{I_2} = 0$), MATLAB returns the following eigenvalues:

$$\lambda_1 = -6.4000 \tag{4.162}$$

$$\lambda_2 = -0.0578 \tag{4.163}$$

$$\lambda_3 = -0.4168 \tag{4.164}$$

$$\lambda_4 = -0.0773 \tag{4.165}$$

All four eigenvalues again have negative real parts thus indicating once more E_0^* as being stable when the drug therapy is active and the immunotherapy is inactive. This is a logical conclusion since the chemotherapy is effective at combating the tumor cells and lowering the over all tumor cell population albeit not as efficiently as the immunotherapy. The next set of eigenvalue calculations is performed when the drug therapy is inactive ($V_C = 0$) and the immunotherapy is active ($V_{I_2} = 10 \times 10^6$). MATLAB returns the following eigenvalues:

$$\lambda_1 = -6.4000 \tag{4.166}$$

$$\lambda_2 = -0.3673 \tag{4.167}$$

$$\lambda_3 = -0.2188 + 0.2743\imath \tag{4.168}$$

$$\lambda_4 = -0.2188 - 0.2743\imath \tag{4.169}$$

All of the eigenvalues have negative real parts once more thus indicating the stability of E_0^* when the drug therapy is inactive and immunotherapy is active. This is a logical conclusion as previous models saw the immunotherapy treatment as being quite effective at reducing the tumor cell population. The final eigenvalue calculation for the first equilibrium point finds both drug therapy and immunotherapy inactive. MATLAB produces the following eigenvalues:

$$\lambda_1 = -6.4000 \tag{4.170}$$

$$\lambda_2 = -0.3300 \tag{4.171}$$

$$\lambda_3 = 0.0327 \tag{4.172}$$

$$\lambda_4 = -0.0730 \tag{4.173}$$

The last scenario with both drug therapy and immunotherapy inactive finds the first equilibrium point E_0^* as unstable, and the tumor cells growing away from $T_0^* = 0$. With no external treatments applied, the tumor cells overwhelm the innate immune system and stabilize to a non-zero population level.

Efforts now focus on the second equilibrium point, E_1^*, to determine its respective stability. Because E_1^* is realized only through numerical calculations, no external treatment parameters are available to change for additonal investigation. Because these treatments are inactive for the majority of the model and when the model is found to stabilize far into the time duration of the model, the treatment parameters are set equal to zero in the calculation of the equilibrium point. The treatment pa-

rameters are also treated as constants in the partial derivative expressions and thus fall out of the expressions very quickly in that process. As such, only one set of eigenvalues is available for E_1^*, and the following eigenvalues represent the situation where both chemotherapy and immunotherapy are inactive. Using the appropriate parameter values [24] along with $V_C = 0$ and $V_{I_2} = 0$, MATLAB produces the following eigenvalues:

$$\lambda_1 = -6.4000 \tag{4.174}$$

$$\lambda_2 = -0.1020 \tag{4.175}$$

$$\lambda_3 = -0.8756 \tag{4.176}$$

$$\lambda_4 = -0.9528 \tag{4.177}$$

With all four eigenvalues having negative real parts, E_1^* is stable, and the tumor cell population tends towards $T_1^* = 1.6657 \times 10^5$. All of the above analysis results are confirmed in the following section through various numerical simulations of the different model scenarios discussed.

4.4.3 Numerical Simulation

As seen in the preceding analyses, this model is a combination of methods previously implemented individually from each other. Both drug therapy and immunotherapy are administered together to investigate the combined efforts and effects of both treatments on the tumor cell population. The first simulation sees both the chemotherapy and immunotherapy as being active ($V_C = 1$ and $V_{I_2} = 10 \times 10^6$).

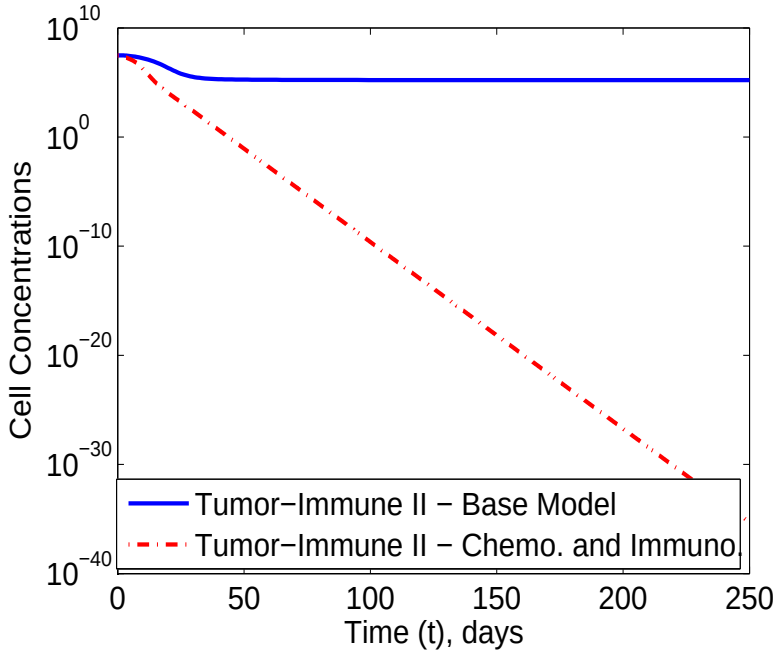

Figure 4.13: Tumor-Immune II - Both Drug Therapy and Immunotherapy Active

With both treatments always active, the tumor cell population quickly declines to a minimum. The simulation confirms the stability of E_0^* when both treatments are active as the tumor cell population does indeed tend towards $T_0^* = 0$. The next simulation finds the drug therapy active but the immunotherapy inactive.

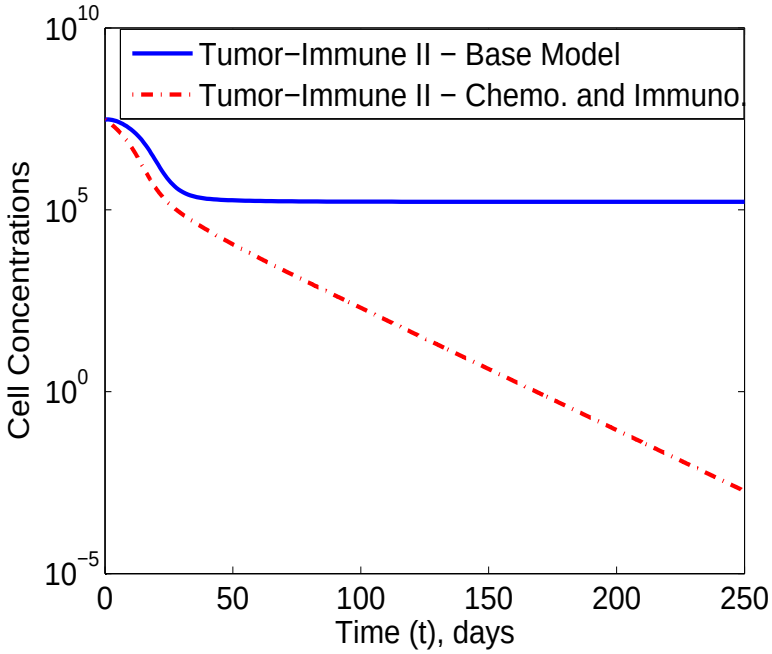

Figure 4.14: Tumor-Immune II - Only Drug Therapy Active

With only the drug therapy active the entire duration of the model, the tumor cell population does decrease to a minimum level but takes a significantly longer amount of time to do so. This simulation confirms the stability of E_0^* even with only one treatment active as seen in the analysis. The next simulation has the drug therapy now inactive and the immunotherapy active.

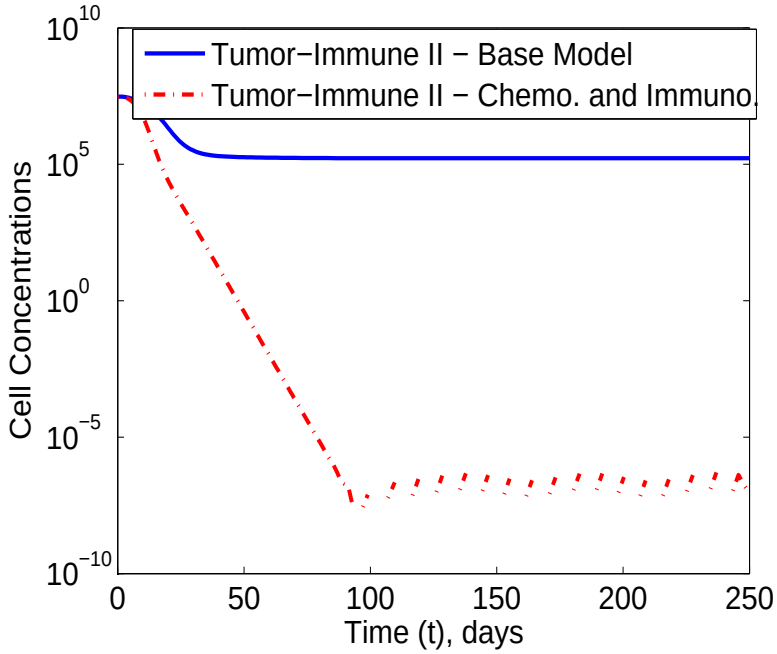

Figure 4.15: Tumor-Immune II - Only Immunotherapy Active

Because the immunotherapy is such a more efficient method at independently combating the cancer cells, this simulation finds the tumor cell population decreasing to a minimum level at a rate very similar to that seen when both treatments were active. Again, this simulation confirms the stability of E_0^* when the immunotherapy is active as seen in the analysis in the previous subsection. The next simulation sees both treatments as inactive.

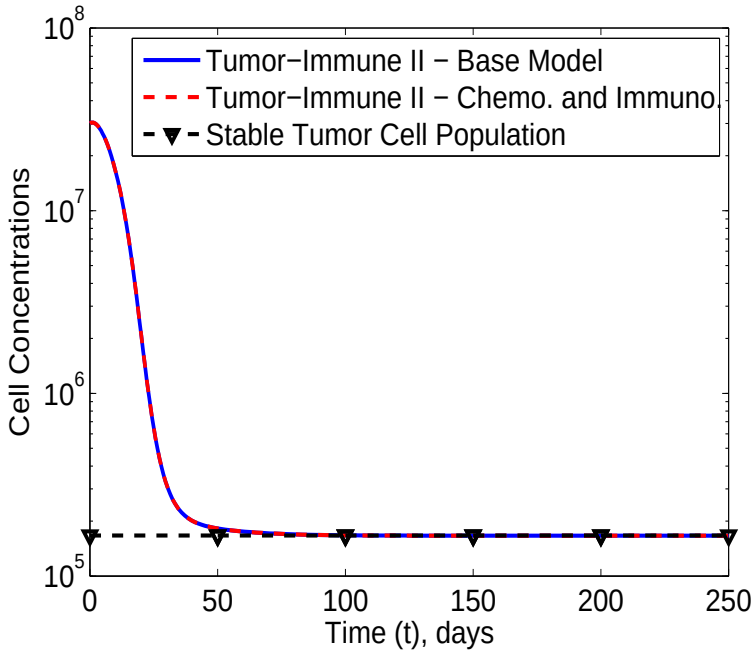

Figure 4.16: Tumor-Immune II - Both Drug Therapy and Immunotherapy Inactive

With both treatments being inactive, the tumor cell population follows the path previously seen in the Tumor-Immune II - Base Model as it stabilizes at a level of $T_1^* = 1.6657 \times 10^5$, thus confirming the instability of E_0^* and stability of E_1^* when both treatments are inactive. The last simulation is more realistic as the treatments are returned to their time-dependent state as opposed to being either always active or always inactive.

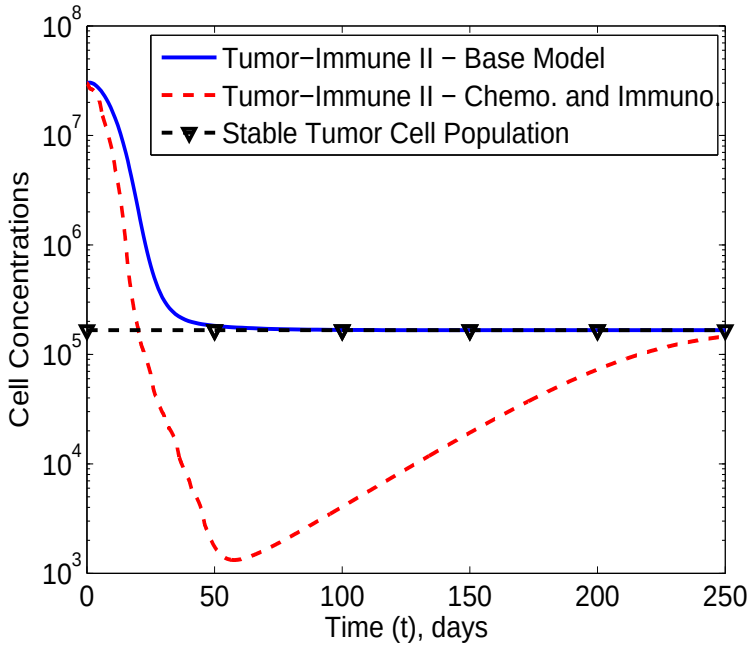

Figure 4.17: Tumor-Immune II - Drug Therapy and Immunotherapy

As seen in the graph of tumor cell population, the simultaneous efforts of both the chemotherapy and immunotherapy when administered as originally intended proved to be better than any previous effort at decreasing the tumor cells during the time in which treatments are active. However, once the treatments turn inactive, the tumor cell population rises yet again to the same stable level observed in the Tumor-Immune II - Base Model simulation. Therefore, while the combined efforts prove to be the most successful, one concurrent dose of each treatment does not decrease the tumor cell population to such levels so as to be considered an overall successful treatment. Further investigation into the manipulation of these treatments is required to find the optimal combination with which to combat the given tumor cell population.

CHAPTER 5

RESULTS AND CONCLUSIONS

5.1 The Best Model and Implementation

Outside of the growth-only model of the tumor cells, this paper discusses two main types of models with subsequent respective iterations and variations. These models range from a basic two-equation interaction model with eventual chemotherapy terms to a three-equation model with eventual chemotherapy, immunotherapy, and subsequent combined terms.

This last variety of model, Tumor-Immune II with drug therapy and immunotherapy, proved to be the most effective at combating the tumor cells present in the host. However, the initial model only ran a simulation of that model with single rounds of chemotherapy and immunotherapy. Obvious realistic treatment options include multiple rounds of either or both supplementary regimens. The limiting nature of a single round of external therapy is seen in the effects on the tumor cells: the tumor cell population eventually returned to the same stable level as in the Tumor-Immune II base model where no external treatments were applied. This level of tumor cell population is not an acceptable value and would hardly classify this model to be realistically worthwhile with its present mode of implementation.

The literature claims the most effective treatment to be chemotherapy followed immediately by immunotherapy [24]. This claim is investigated by modulating the order, frequency, and duration of the chemotherapy and immunotherapy treatments while monitoring the tumor cell and immune cell levels to determine which combina-

tion of treatments results in an acceptable implementation of the model as defined by the respective cell populations. Generally speaking, the overall goal is to minimize the tumor cell population while simultaneously maximizing the immune cell population within the parameters of the model. As seen in the model analysis, the chemotherapy obviously affects both types of cells, hence the need to find the balance between treatments.

5.2 Further Implementations

5.2.1 Single Dose Models

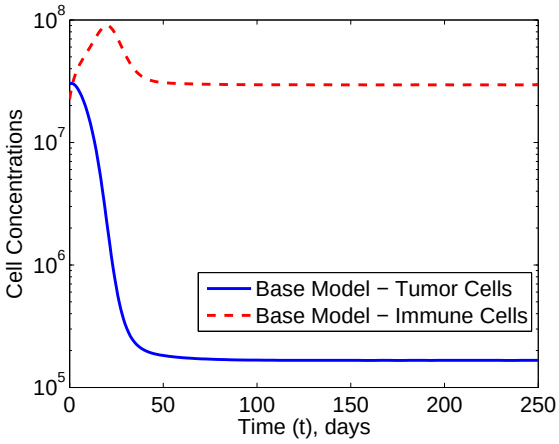

Figure 5.1: Tumor-Immune II - Base Model

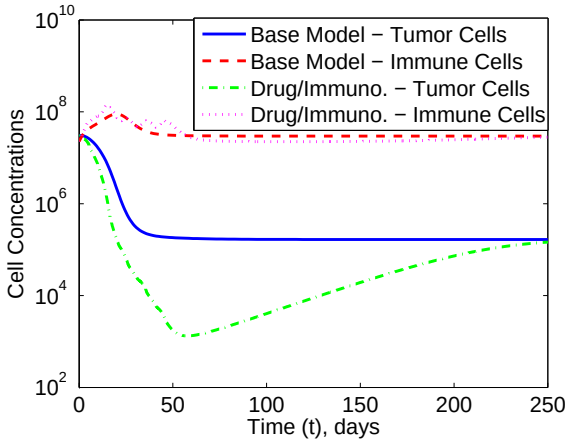

Figure 5.2: Tumor-Immune II - Concurrent Treatments

By observing the simulations, it is easily seen that while each model has varying results, none of them achieve a substantially low level of tumor cells for a sizable length of time. Interestingly enough, the immune cell population counts are very similar among all simulations with cyclical patterns in population levels only occurring during

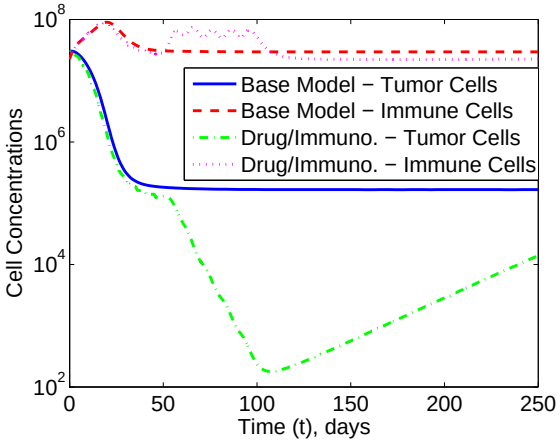

Figure 5.3: Tumor-Immune II - Drug Therapy then Immunotherapy

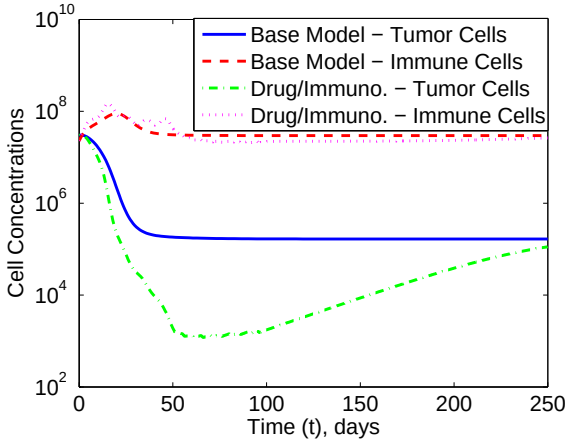

Figure 5.4: Tumor-Immune II - Immunotherapy then Drug Therapy

the immunotherapy treatment. Once all treatments end, the immune cell population stabilizes to levels observed with the Tumor-Immune II - Base Model.

Figures (5.2) and (5.4) resulted in very similar results, with the model described by Figure (5.4) being more effective at maintaining lower levels of tumor cells for a longer period of time (≈ 50 days). Figure 5.3 demonstrates what could be considered the worst performance of these three variations with respect to time as the lowest concentration of tumor cells was not realized until approximately 100 days after external treatment began. Ironically, this is the order of treatments described in [24] as being the most effective. This was, however, but one single dose of each treatment. Simulations below demonstrate the effectiveness of multiple doses in varying orders.

5.2.2 Multiple Dose Models

The first multiple dose model in Figure (5.5) finds two concurrent treatments implemented back to back. That is, the drug therapy and immunotherapy is administered together until each treatment ends, and then another identical treatment of

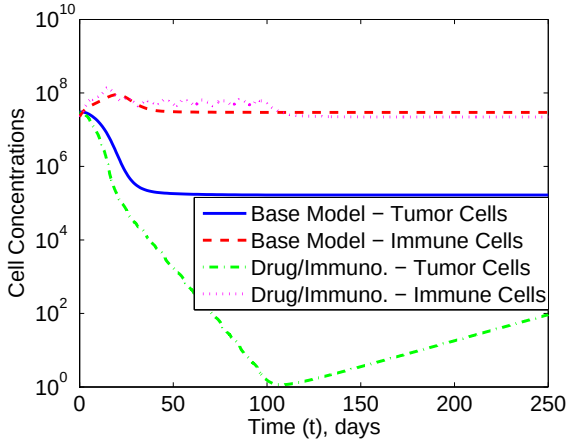

Figure 5.5: Tumor-Immune II - Two Concurrent Doses of Drug Therapy and Immunotherapy

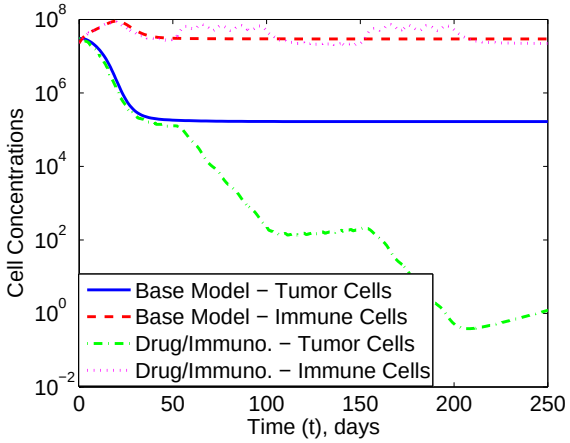

Figure 5.6: Tumor-Immune II - Two Doses Each, Drug Therapy then Immunotherapy

both therapies is started immediately after the first. While the model shows this to be the most effective option, the reality of such a course of action is rather inhibitory. The immune cells did not deviate substantially from the stable level of of the Tumor-Immune II - Base Model, but that cannot be the only litmus test of a viable treatment option. Chemotherapy affects many more aspects of a host's life and is difficult on the patient in general. While any potentially undesireable side affects of the immunotherapy are not discussed in the literature germane to this work, one must consider the negative aspects of successive rounds of drug therapy and not consider the first multiple dose model as a possible treatment option.

Taking into account the possible side effects on the host unaccounted for by the simulations, the second model in Figure (5.6) demonstrates one round of drug therapy followed immediately by a round of immunotherapy. Once the immunotherapy is finished, a second dose of drug therapy is administered followed immediately once again by a second round of immunotherapy. The immune cells oscillate around the

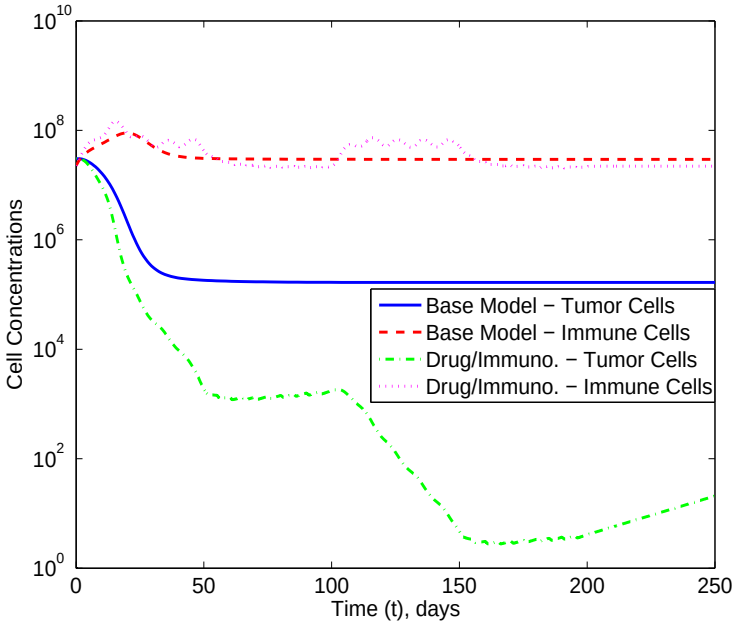

Figure 5.7: Tumor-Immune II - Two Doses Each, Immunotherapy then Drug Therapy

steady state level of the base model depending on the activation or inactivation of the immunotherapy treatment.

The final simulated model in Figure (5.7) is motivated similarly to the second simulation. That is, the model attempts to mitigate any possible side effects of one external treatment or the other by alternating both of them for the course of two doses each such that only one therapy is active at a time. This time, however, finds the immunotherapy administered first followed by the chemotherapy. While the minimum amount of tumor cells does not fall as low as the second model, this minimum is reached approximately 30 days prior to the minimum attained in the second model. Observing the behavior of the models with respect to the tumor cell population levels along with fluctuations in immune cell counts, the final simulation represented by Figure (5.7) appears to be the most efficient with regard to the order

of therapies. This contradicts what is claimed in the literature [24], but the respective article making that claim only administered a single round of each specific therapy.

5.3 Future Investigations

Despite having observed a plausible solution to this specific tumor cell population, much more research is obviously necessitated in this field as more and more biological information becomes available about the variety of different tumors and how they react, different treatments and therapies and how efficient they are, and how the innate system continues to react to not only the tumor but also the treatment options, etc. One such area of interest is that of tumor vaccine treatment [24] [42] as well as additional immunotherapy involving a separate substance called $TGF-\beta$ [42]. There exists recent research into these two topics, but the interesting question remains of combining those treatment options alongside the ones discussed in this paper. This area of interest could also be expanded by investigating and designing a cellular automata model to take into account not only the temporal effects of the model but also the spatial aspects as well. Designing any of the aforementioned models as stochastic instead of being purely deterministic is also a potential area of interest to perhaps better investigate the true dynamics of the tumor and its environment in the host system.

APPENDIX A

TABLES OF IMPORTANT VALUES

Table A.1: Values to Model Coefficients

Coefficient	Units	Value	Description	Source
a_0	day^{-1}	0.13	tumor growth rate	[24]
b	cells^{-1}	2.3×10^{-9}	reciprocal carrying capacity	[24]
c_0	$\text{cells}^{-1}\ \text{day}^{-1}$	4.4×10^{-9}	tumor cell kill rate by immune cells	[24]
d	cells day^{-1}	7.3×10^{6}	CTL immune cell induction rate	[24]
e	$\text{cells}^{-1}\ \text{day}^{-1}$	9.9×10^{-9}	CTL proliferation rate induced by IL-2	[24]
f	day^{-1}	0.33	CTL immune cell death rate	[24]
g	unit day^{-1}	1.6×10^{7}	antigen presentation	[24]
j	$\text{cells}^{-1}\ \text{day}^{-1}$	3.3×10^{-9}	rate of consumption of IL-2 by CTL	[24]
k	$\text{cells}^{-1}\ \text{day}^{-1}$	1.8×10^{-8}	inactivation of IL-2 molecules	[24]
l	cell	3×10^{6}	half-saturation constant	[24]
M_L	day^{-1}	0.6	CTL immune cell kill rate via chemotherapy	[24]
M_T	day^{-1}	0.9	tumor cell kill rate via chemotherapy	[24]
p	day^{-1}	6.4	decay rate of chemotherapy	[24]
V_C	dose day^{-1}	1	chemotherapy induction rate	[24]
V_{I_2}	MU day^{-1}	10×10^{6}	immunotherapy induction rate	[24]

Table A.2: Values to Various Initial Cell Populations

Variable	Value	Description	Source
T_0	3×10^{7}	Tumor Cells	[24]
L_0	2.25×10^{7}	CTL Immune Cells	[24]
C_0	0	Chemotherapy Drug Concentration	[24]
I_{2_0}	2.4×10^{7}	$IL-2$ molecules	[24]

REFERENCES

[1] Rosemary J Akhurst and Rik Derynck. TGF-β signaling in cancer–a double-edged sword. *Trends in cell biology*, 11(11):S44–S51, 2001.

[2] Nicola Bellomo and Luidgi Preziosi. Modelling and mathematical problems related to tumor evolution and its interaction with the immune system. *Mathematical and Computer Modelling*, 32(3):413–452, 2000.

[3] Marc Beyer and Joachim L Schultze. Regulatory T cells in cancer. *Blood*, 108(3):804–811, 2006.

[4] José L Boldrini and Michel Is Costa. Therapy burden, drug resistance, and optimal treatment regimen for cancer chemotherapy. *Mathematical Medicine and Biology*, 17(1):33–51, 2000.

[5] H.M. Byrne. Using mathematics to study solid tumour growth. In *Proceedings of the 9th General Meetings of European Women in Mathematics*, pages 81–107, 2000.

[6] HM Byrne and SA Gourley. The role of growth factors in avascular tumour growth. *Mathematical and Computer Modelling*, 26(4):35–55, 1997.

[7] Dennis L Chao, Miles P Davenport, Stephanie Forrest, and Alan S Perelson. A stochastic model of cytotoxic t cell responses. *Journal of Theoretical Biology*, 228(2):227–240, 2004.

[8] M.A.J. Chaplain. Avascular growth, angiogenesis and vascular growth in solid tumours: The mathematical modelling of the stages of tumour development. *Mathematical and Computer Modelling*, 23:47–87, March 1996.

[9] L.G. de Pillis and A. Radunskaya. The dynamics of an optimally controlled tumor model: A case study. *Mathematical and Computer Modelling*, 37:1221–1244, June 2003.

[10] Lisette G de Pillis, Weiqing Gu, K Renee Fister, TA Head, K Maples, A Murugan, T Neal, and K Yoshida. Chemotherapy for tumors: An analysis of the dynamics and a study of quadratic and linear optimal controls. *Mathematical Biosciences*, 209(1):292–315, 2007.

[11] Lisette G de Pillis, Weiqing Gu, and Ami E Radunskaya. Mixed immunotherapy and chemotherapy of tumors: modeling, applications and biological interpretations. *Journal of theoretical biology*, 238(4):841–862, 2006.

[12] Lisette G. de Pillis, Ami E. Radunskaya, and Charles L. Wiseman. A validated mathematical model of cell-mediated immune response to tumor growth. *Cancer Research*, 65:7950–7958, Sept 2005.

[13] Said Dermime, Anne Armstrong, Robert E Hawkins, and Peter L Stern. Cancer vaccines and immunotherapy. *British medical bulletin*, 62(1):149–162, 2002.

[14] Rik Derynck, Rosemary J Akhurst, and Allan Balmain. Tgf-β signaling in tumor suppression and cancer progression. *Nature genetics*, 29(2):117–129, 2001.

[15] Martin Eisen. *Mathematical models in cell biology and cancer chemotherapy*, volume 30. Springer Science & Business Media, 2013.

[16] B Firmani, L Guerri, and Luigi Preziosi. Tumor/immune system competition with medically induced activation/deactivation. *Mathematical Models and Methods in Applied Sciences*, 9(04):491–512, 1999.

[17] Judah Folkman and Mark Hochberg. Self-regulation of growth in three dimensions. *The Journal of experimental medicine*, 138(4):745–753, Oct 1973.

[18] Center for Disease Control and Prevention. Deaths: Final data for 2013.

[19] Ricardo P Garay and René Lefever. A kinetic approach to the immunology of cancer: Stationary states properties of efffector-target cell reactions. *Journal of Theoretical Biology*, 73(3):417–438, 1978.

[20] Silvia Garbelli, Stefania Mantovani, Belinda Palermo, and Claudia Giachino. Melanocyte-specific, cytotoxic t cell responses in vitiligo: the effective variant of melanoma immunity? *Pigment cell research*, 18(4):234–242, 2005.

[21] J.G. Garnier and A. Quételet. *Correspondance mathématique et physique*. Impr. d'H. Vandekerckhove, Brussels, 1838.

[22] HP Greenspan. Models for the growth of a solid tumor by diffusion. *Stud. Appl. Math*, 51(4):317–340, 1972.

[23] Zhiwei Hu, Ying Sun, and Alan Garen. Targeting tumor vasculature endothelial cells and tumor cells for immunotherapy of human melanoma in a mouse xenograft model. *Proceedings of the National Academy of Sciences*, 96(14):8161–8166, 1999.

[24] O.G. Isaeva and V.A. Osipov. Different strategies for cancer treatment: Mathematical modelling. *Computational and Mathematical Methods in Medicine*, 10:253–272, Dec 2009.

[25] Denise Kirschner and John Carl Panetta. Modeling immunotherapy of the tumor–immune interaction. *Journal of Mathematical Biology*, 37(3):235–252, 1998.

[26] Vladimir A Kuznetsov and Gary D Knott. Modeling tumor regrowth and immunotherapy. *Mathematical and Computer Modelling*, 33(12):1275–1287, 2001.

[27] Amy H Lin. A model of tumor and lymphocyte interactions. *Discrete and Continuous Dynamical Systems Series B*, 4(1):241–266, 2004.

[28] D.G. Mallet and L.G. De Pillis. A cellular automata model of tumor-immune system interactions. *Journal of Theoretical Biology*, 239:334–350, Sept 2005.

[29] Thomas Malthus. *An Essay on the Principle of Population*. J. Johnson, London, 1798.

[30] Anastasios Matzavinos, Mark AJ Chaplain, and Vladimir A Kuznetsov. Mathematical modelling of the spatio-temporal response of cytotoxic t-lymphocytes to a solid tumour. *Mathematical Medicine and Biology*, 21(1):1–34, 2004.

[31] S Michelson and JT Leith. Host response in tumor growth and progression. *Invasion & metastasis*, 16(4-5):235–246, 1995.

[32] JC Panetta. A logistic model of periodic chemotherapy with drug resistance. *Applied Mathematics Letters*, 10(1):123–127, 1997.

[33] John Carl Panetta. A mathematical model of periodically pulsed chemotherapy: tumor recurrence and metastasis in a competitive environment. *Bulletin of Mathematical Biology*, 58(3):425–447, 1996.

[34] CP Please, GJ Pettet, and DLS McElwain. Avascular tumour dynamics and necrosis. *Mathematical Models and Methods in Applied Sciences*, 9(04):569–579, 1999.

[35] Lambert Adolphe Jacques Quetelet. *Sur lhotntne et le developpetnent de ses faciiltes, ou essai de physique sociale*. Bachelier, Paris, 1835.

[36] Tiina Roose, S. Jonathan Chapman, and Philip K. Maini. Mathematical models of avascular tumor growth. *SIAM Review*, 49:179–208, May 2007.

[37] American Cancer Society. The history of cancer, June 2014.

[38] Akulapalli Sudhakar. History of cancer, ancient and modern treatment methods. *Journal of Cancer Science & Therapy*, 1:1–4, Dec 2009.

[39] Vinay G Vaidya and Frank J Alexandro. Evaluation of some mathematical models for tumor growth. *International Journal of Bio-Medical Computing*, 13(1):19–35, 1982.

[40] John P Ward and JR King. Mathematical modelling of avascular-tumour growth. *Mathematical Medicine and Biology*, 14(1):39–69, 1997.

[41] JP Ward and JR King. Mathematical modelling of avascular-tumour growth ii: modelling growth saturation. *Mathematical Medicine and Biology*, 16(2):171–211, 1999.

[42] Shelby Wilson and Doron Levy. A mathematical model of the enhancement of tumor vaccine efficacy by immunotherapy. *Bulletin of Mathematical Biology*, 74:1485–1500, July 2012.

[43] Yongzhi Xu. A free boundary problem model of ductal carcinoma in situ. *Discrete and Continuous Dynamical Systems Series B*, 4(1):337–348, 2004.

BIOGRAPHICAL STATEMENT

Robert P Childress was born in Fort Worth, TX in 1984. He received his B.S. degree in Computer Science from Texas A&M University (College Station, TX) in 2008 and his M.S. degree in Mathematics from the University of Texas at Arlington (Arlington, TX) in 2015. From 2009 to 2013 he was employed by Tarrant County College as an Instructional Associate in the Math Resource Center. In 2014 he joined the University of Texas at Arlington as the Learning Resource Coordinator in the Math Emporium Lab. His current work includes collecting and analyzing student performance data and creating student success forecast models for the service level mathematics courses.